FREQUENCY ANALYSIS OF UNDERWATER
EXPLOSIONS IN GAS-WATER RESONATOR.
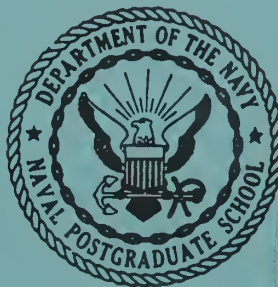
Allen D. Keimig

UNITED STATES
NAVAL POSTGRADUATE SCHOOL

THESIS

FREQUENCY ANALYSIS OF UNDERWATER EXPLOSIONS

IN A GAS - WATER RESONATOR

* * * * * * * *

Allen D. Keimig, Jr.
and
John L. Hofmockel

FREQUENCY ANALYSIS OF UNDERWATER EXPLOSIONS

IN A GAS - WATER RESONATOR

* * * * * * * *

Allen D. Keimig, Jr.

and

John L. Hofmockel

FREQUENCY ANALYSIS OF UNDERWATER EXPLOSIONS

IN A GAS - WATER RESONATOR

by

Allen D. Keimig, Jr.

Lieutenant, United States Navy

and

John L. Hofmockel

Lieutenant Commander, United States Navy

Submitted in partial fulfillment of
the requirements for the degree of

MASTER OF SCIENCE
IN
ENGINEERING ELECTRONICS

United States Naval Postgraduate School
Monterey, California

1961

UNCLASSIFIED

FREQUENCY ANALYSIS OF UNDERWATER EXPLOSIONS

IN A GAS – WATER RESONATOR

by

Allen D. Keimig, Jr.

and

John L. Hofmockel

This work is accepted as fulfilling

the thesis requirements for the degree of

MASTER OF SCIENCE

IN

ENGINEERING ELECTRONICS

from the

United States Naval Postgraduate School

UNCLASSIFIED

ABSTRACT

This thesis presents the results of an experimental investigation of the frequency spectrum of the acoustic output from underwater explosions in a gas-water resonator. Measured amounts of hydrogen, oxygen, and nitrogen were used as an explosive charge in cylindrical containers and fired at depths between 25 and 200 feet. Excess unburned gas remaining in the container caused the sound to be concentrated in certain low frequencies; these frequencies correspond closely to predictions based on Helmholtz Resonator calculations. The spectrum was influenced by surface reflection and by frequency shifts observed during the explosive pulse. A narrow band low frequency spectrum analysis system is described.

UNCLASSIFIED

CONFIDENTIAL

TABLE OF CONTENTS

UNCLASSIFIED

LIST OF ILLUSTRATIONS

UNCLASSIFIED

LIST OF ILLUSTRATIONS

UNCLASSIFIED

LIST OF ILLUSTRATIONS

vi

UNCLASSIFIED

1. Introduction

Underwater explosions of a mixture of hydrogen and oxygen gases
produced by electrolysis of sea water have been described as a high power
source of acoustic waves by previous experimenters $\underline{/1/}$, $\underline{/2/}$. Qualita-
tive results obtained by Harris and Rigsbee $\underline{/1/}$ showed that the acoustic
pulses produced by such explosions could have varying pulse lengths and
spectral characteristics under different conditions of gas mixtures and
depths.

The intent of the present authors was to find a functional relation
of mixture and depth to the frequency spectrum of the acoustic pulses
from underwater hydrogen-oxygen explosions. The ability to reproduce
and predict a particular frequency spectrum would have obvious value.
It would then be possible to employ a narrow band receiver for detecting
echoes.

Inherent in the problem of studying the frequency components con-
tained in the pulses was the problem of development of a narrow band
frequency analyzer. Preliminary work indicated that it would be possible
to build a narrow band system for use at low audio frequencies. Con-
siderable time and effort was expended in the development of the fre-
quency analyzer. In its final form it had a band width of 2.25 cycles
per second, was flat within one decibel from 20 cycles per second to
2500 cycles per second, and had a dynamic range of 25 decibels. Its

output was in the convenient form of a graphical plot of sound pressure spectrum level as a function of frequency. A complete description of the frequency analyzer design and operation is included in Appendix I.

The production of hydrogen and oxygen by electrolysis of sea water at various depths and temperatures introduces unknown variability in gas quantity and hydrogen to oxygen mixture. For precise analysis it was decided to use measured quantities of gas. Tanks of compressed gas were used as a source, and a scheme was devised whereby the explosive chamber could be loaded just below the surface of the water at very nearly one atmosphere. Close control of the total volume of gas as well as the ratios was possible. Appendix II provides a more thorough discussion of the apparatus and metering method used.

An investigation of water-air filled resonators by V. I. Sorokin /3/ indicated that it is possible to have an underwater resonator of low audio frequency and relatively small dimensions. Analysis of the resonator showed that the resonant frequency was dependent on the density and speed of sound in the trapped gas as well as the volume. To investigate the possibility that such a resonance condition could be excited by explosion and the frequency varied by varying the volume and kinds of gases remaining after the explosion, the authors decided to use varying quantities of extra hydrogen and nitrogen in the combustion chamber.

Work was conducted entirely at the U. S. Naval Postgraduate School, Monterey, California. All acoustic measurements were made in Monterey Bay in water ranging from 200 feet to 250 feet in depth. A series of 80 explosions at depths from the surface to 200 feet were recorded and frequency analyzed.

We wish to express our appreciation to Professor L. R. Kinsler, Professor D. A. Stentz, and Captain Louis Spear, USN, of the U. S. Naval Postgraduate School for their advice and encouragement.

2.   Measurements

Test signals were made by igniting explosive mixtures of hydro-
gen, oxygen, and nitrogen gases underwater in cylindrical transducers.
The mixture of gases was ignited by heating a length of nichrome wire
at the top of the transducer. The transducer was loaded with measured
quantitities of the gases; a description of the technique employed in
measuring the gases appears in Appendix II. The loaded transducer was
lowered to the firing depth after loading, and a current of 12 to 15 amp-
eres passed through the conductors to the nichrome wire.

The sound produced by the explosion was received by a barium
titanate hydrophone located 40 feet horizontally from the transducer.
The electrical signal from the hydrophone was recorded on an Ampex
600 Tape Recorder.

The resulting magnetic tapes were played back to a Hughes
Memoscope and photographs taken of the time trace of each explosion.
Then the signals were processed through the spectrum analyzer. Refer
to Appendix I for a complete description of the spectrum analyzer.

Throughout the following discussion, reference will be made to
the spectral plots and the time pictures of the explosions. In every case
the frequency scale across the bottom begins at ten cycles per second.
Vertical lines mark each ten cycles up to 100 cycles per second; above
100 cycles per second the vertical lines mark each multiple of 100 cycles

per second. The horizontal lines indicate relative spectrum level. The

darker horizontal lines are spaced five decibels apart. The spectrum

levels are relative only for the components within a given spectrum and

there is no reference level for comparison between individual pictures.

No attempt was made to compare the intensity of different explosions

because there was no way to know the exact distance between the trans-

ducer and hydrophone at any time. There was also no calibration of the

hydrophone as to the influence of hydrostatic pressure differences.

All time pictures have the time scale of 20 milliseconds per

division except a few which are recorded at 10 milliseconds per division

to improve the display. The exceptions are noted in the figures. The

spectrum analyzer has a range up to 2500 cycles per second but where

no components appear above a certain frequency the spectral plots have

been cut off for convenience of presentation.

3.   Effect of Excess Hydrogen

A stoichiometric mixture of two parts hydrogen and one part oxygen by volume produced a broad spectrum, nearly continuous in the range 20 to 100 cycles per second, with components extending out to 800 cycles per second for the deeper explosions. (See Figures 1(a), 2(a), 3(a), and 4(a).) As the amount of hydrogen was increased certain low frequency components appeared to be enhanced compared to the higher frequency components.

Figure 1 shows four explosions at a depth of 50 feet, starting with a stoichiometric mixture ratio in figure 1(a). In Figures 1(b), 1(c), and 1(d) the amount of hydrogen was increased. The explosion in Figure 1(d) had 3.0 liters excess hydrogen and shows a marked tendency toward a line spectrum. It can be observed that the frequency components which appear so pronounced in Figure 1(d) also appear less pronounced but at the same frequencies in 1(a), 1(b), and 1(c). The component at 110 cycles per second is clearly visible in all four spectra.

The same tendency can be observed in Figure 2 which shows the spectra of four explosions at 100 feet depth. Components visible in Figure 2(d) can be traced in the other spectra, especially the components near 40 and 100 cycles per second. With less hydrogen, additional components appear, filling in the gaps, until in the explosion of Figure 2(a), the spectrum is continuous and nearly flat up to 100 cycles per second.

(a) 6.45 liter transducer
Depth 50 feet
H_2 : 0.67 liter
O_2 : 0.33 liter

(b) 6.45 liter transducer
Depth 50 feet
H_2 : 1.67 liter
O_2 : 0.33 liter

(c) 6.45 liter transducer
Depth 50 feet
H_2 : 2.67 liter
O_2 : 0.33 liter

(d) 6.45 liter transducer
Depth 50 feet
H_2 : 3.67 liter
O_2 : 0.33 liter
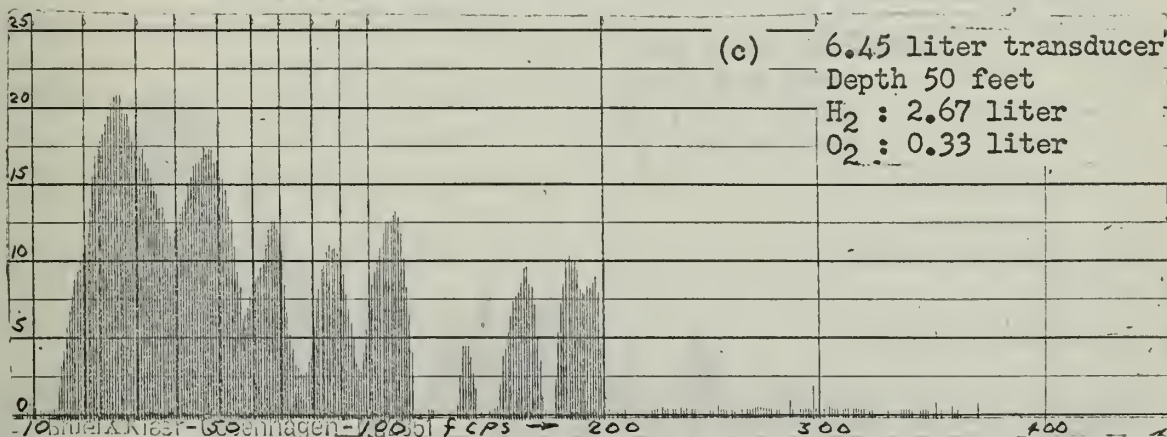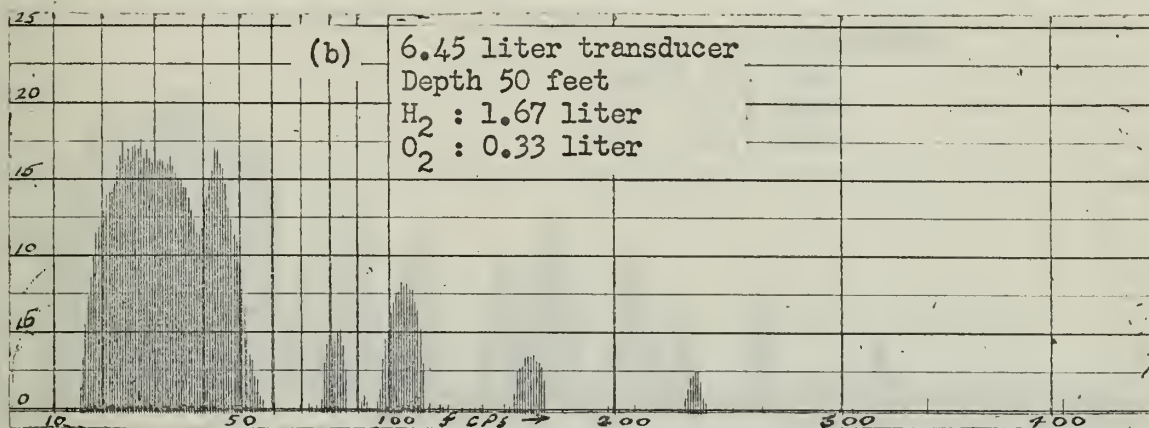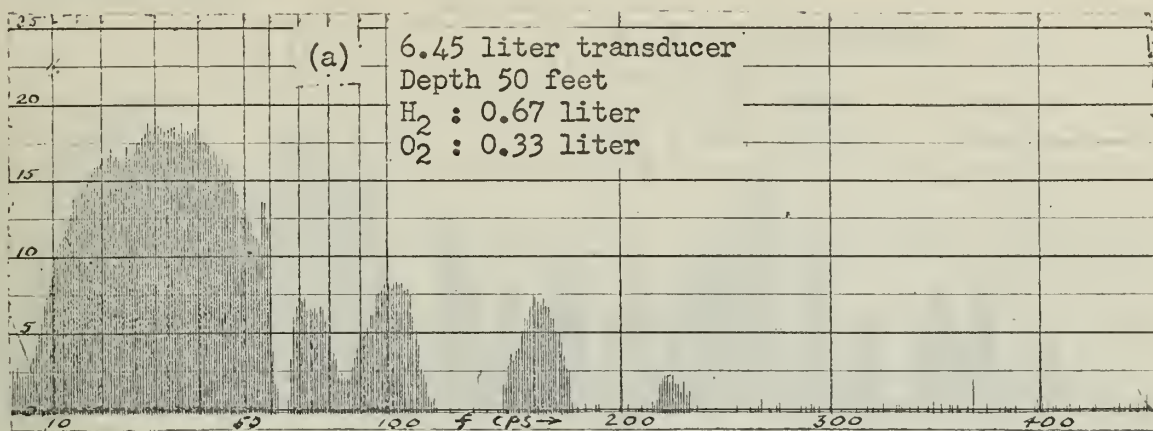
Fig. 1 Spectrum as a Function of Varying Excess H_2, Depth 50 ft.

Fig. 2 Spectrum as a Function of Varying Excess H_2, Depth 100 ft.

At a depth of 150 feet Figure 3 shows the same tendency. In-creasing hydrogen produces a pronounced enhancement of the 43 cycle per second component. At the same time there is a complete elimination of the strong components in the 200 to 300 cycle per second range which were present in Figure 3(a), the stoichiometric mixture.

The spectra of Figure 4, explosions at 200 feet depth, show the same tendencies previously associated with increasing hydrogen, that is, suppression of higher frequency components accompanied by raising of certain components.

We can note that there is a persistence of some components; for any given depth these components maintain a fixed frequency through-out the range of increasing hydrogen. While there is no apparent change in the frequencies of the individual components, there is a shift of the acoustical energy to certain enhanced components. These enhanced components invariably appear in the lower frequency range.

As is well known, a pulse of a cosine wave of duration T and frequency f_0 has an amplitude spectrum described by the factor;

$$\frac{T}{2} \frac{\sin (\omega - \omega_o) \frac{T}{2}}{(\omega - \omega_o) \frac{T}{2}}$$

This is a $\frac{\sin x}{x}$ spectrum centered at ω_o and since it falls off to zero where $(\omega - \omega_o) \frac{T}{2} = \pi$, $f - f_0 = \frac{1}{T}$ for the first zero of the $\frac{\sin x}{x}$ curve. It takes a long pulse to produce a narrow spectrum and the broad
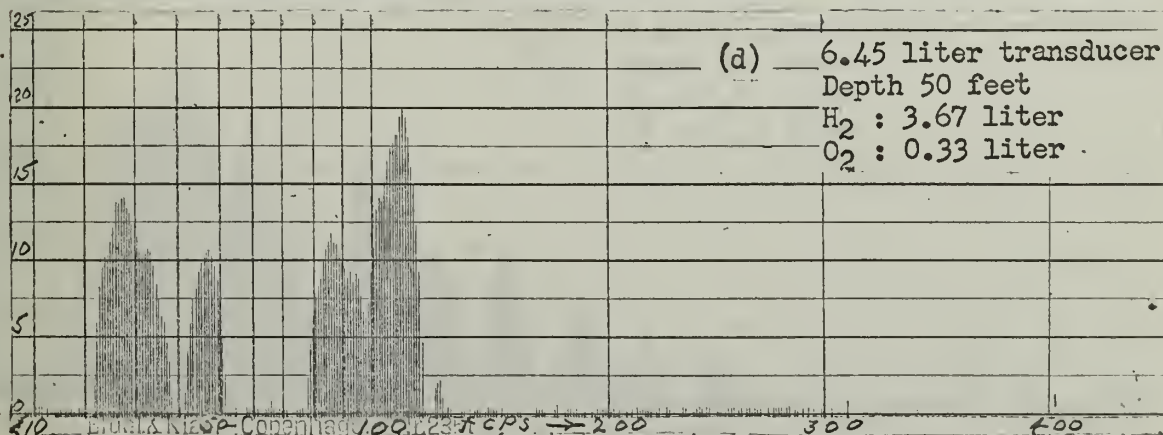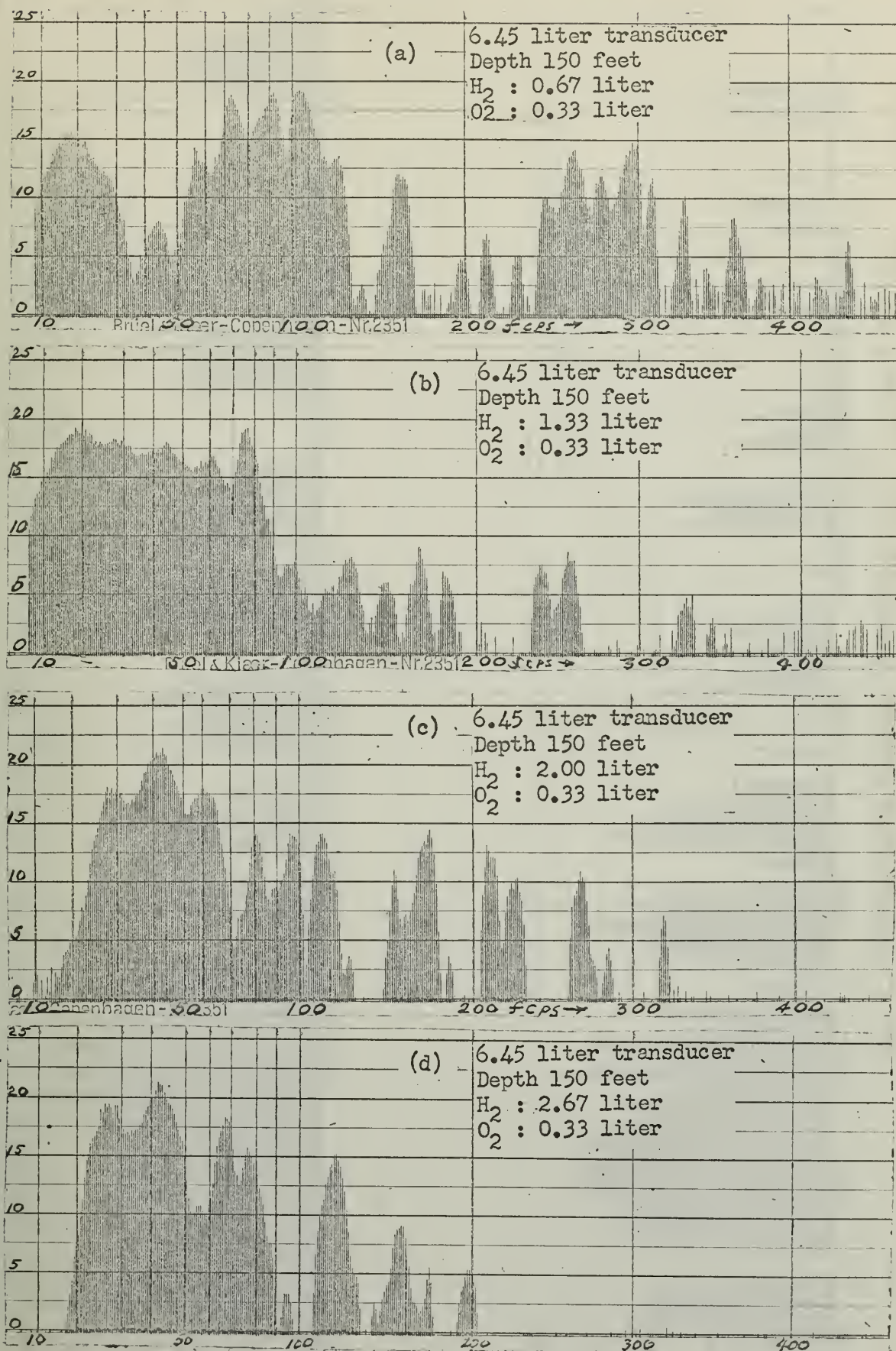
Fig. 3 Spectrum as a Function of Varying Excess H_2, Depth 150 ft.

(a) 6.45 liter transducer
Depth 200 feet
H_2 : 0.67 liter
O_2 : 0.33 liter

(b) 6.45 liter transducer
Depth 200 feet
H_2 : 1.33 liter
O_2 : 0.33 liter
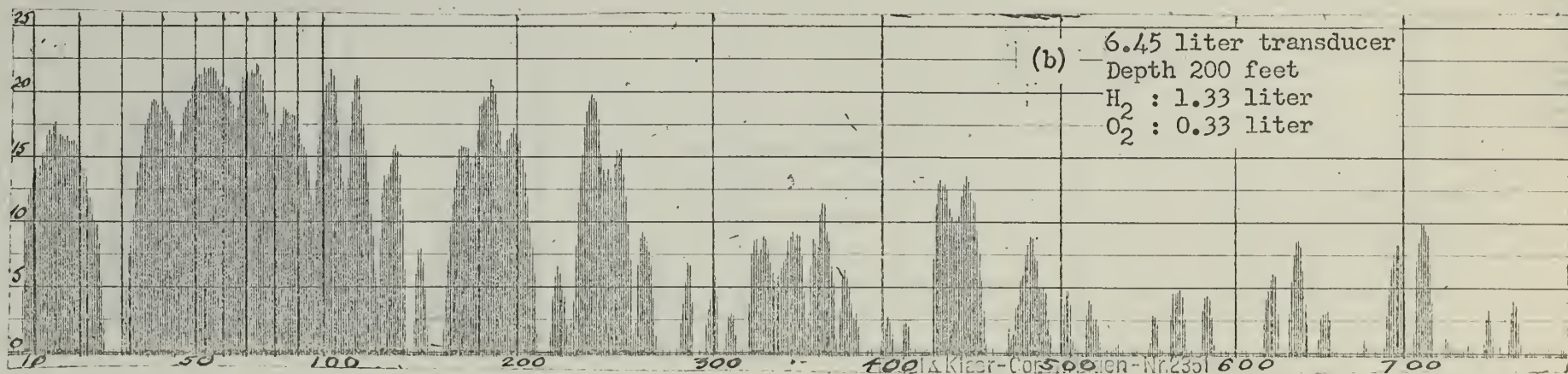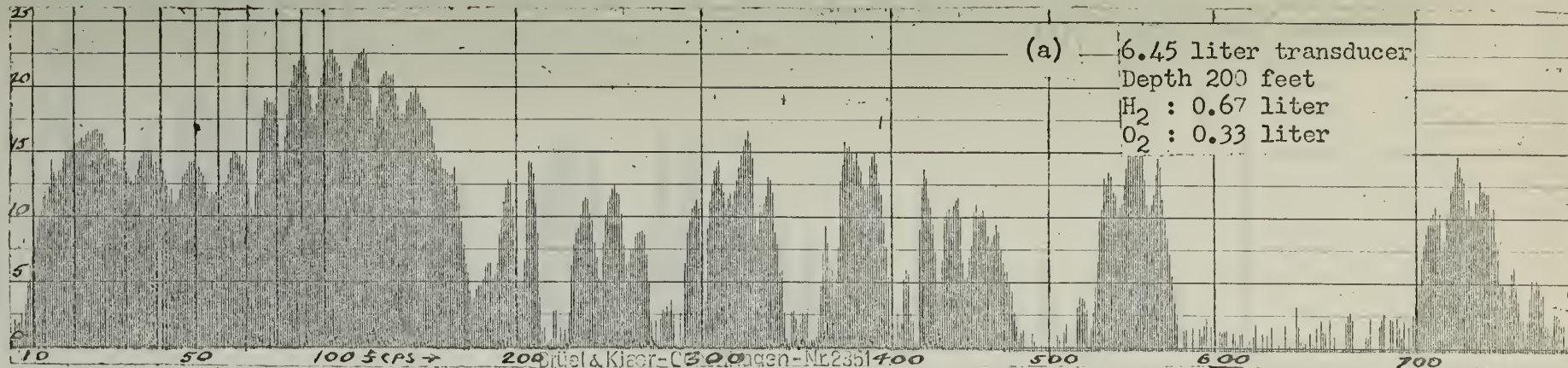
Fig. 4   Spectrum as a Function of Varying Excess H_2, Depth 200 ft.

(c) 6.45 liter transducer
Depth 200 feet
H_2 : 2.00 liter
O_2 : 0.33 liter

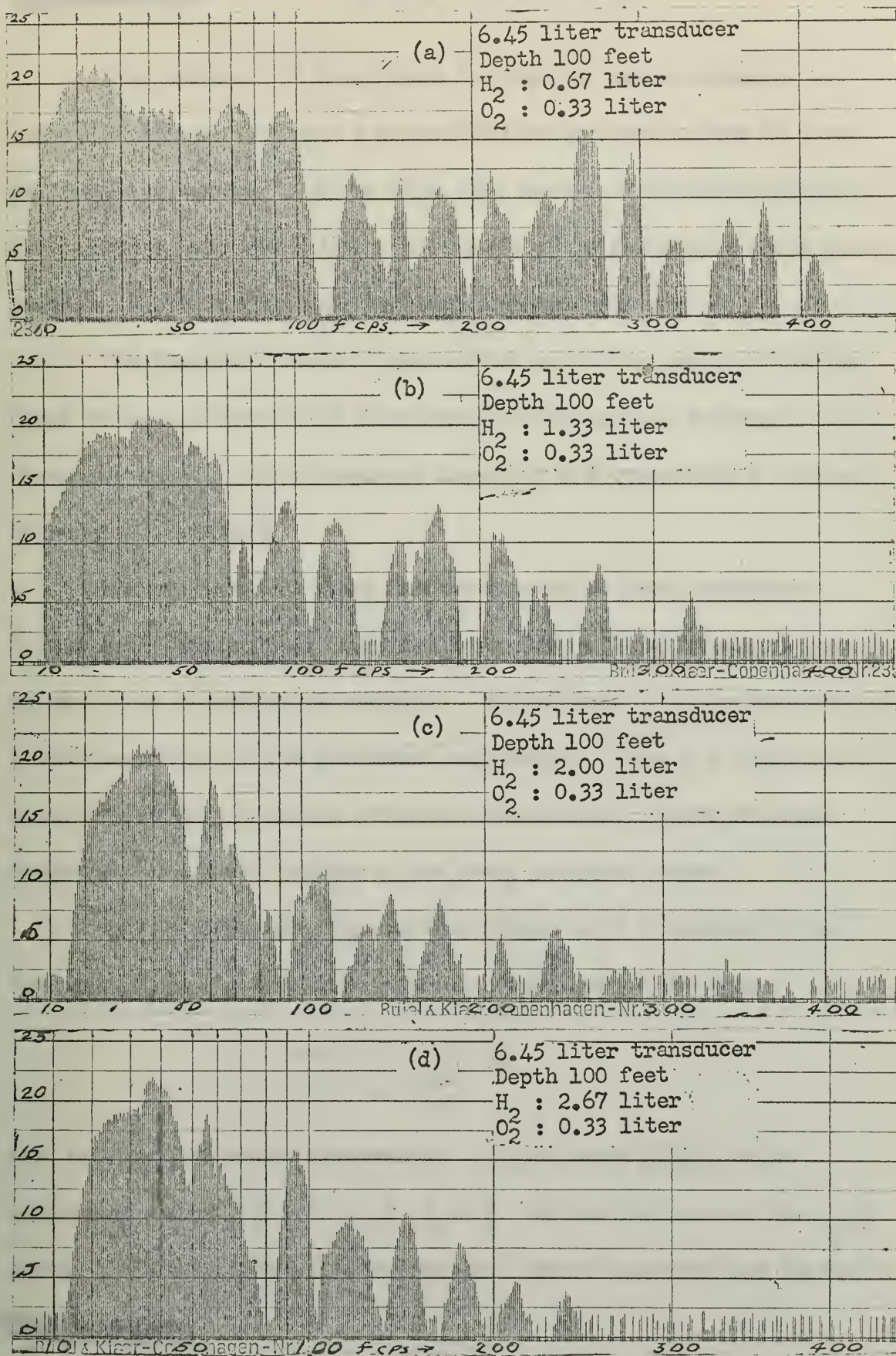(d) 6.45 liter transducer
Depth 200 feet
H_2 : 2.67 liter
O_2 : 0.33 liter

Fig. 4

12
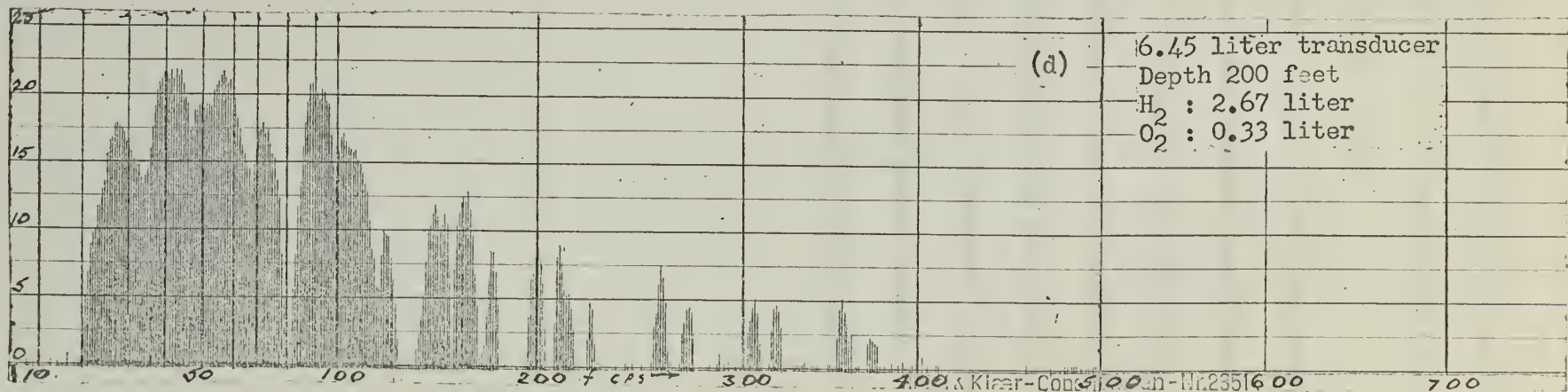
CONFIDENTIAL

humped spectra of Figures 1 through 4 are produced by relatively short

pulses of the frequencies. Some 60 cycle per second hum of long dura-

tion can be seen in figure 1(a) as a very narrow spike.

Suppose an explosion contained short pulses of two frequencies

close together so that their $\frac{\sin x}{x}$ spectral distributions overlapped.

It would then be possible for the spectral components from the two pulses

to add, and, depending upon the phase relation of the two frequencies,

produce either a third spectral spike of higher amplitude than the indi-

vidual frequencies or a narrow gap between the two fundamental frequen-

cies. Such a possibility must always be considered when viewing a

spectrum such as Figure 3(a) which shows three peaks close together.

CONFIDENTIAL

4.   Effect of Added Nitrogen

Further investigations of the effects of excess gas in the ignition
chamber involved the use of nitrogen. Nitrogen is inert and does not
enter into the chemistry of the explosion. One liter of a stoichiometric
mixture of hydrogen and oxygen was used as the basic explosive charge.
Additional amounts of nitrogen were placed in the chamber as the varying
parameter. Figure 5 shows the effect at 50 feet depth of increasing
amounts of nitrogen. Evidently the increased nitrogen produced the same
sort of trends as increased hydrogen. For example, three liters of excess
nitrogen produced, as shown in Figure 5(d), very strong components at 25,
44, 70, and 100 cycles per second. The narrowing spikes are the result
of increasing pulse duration.

Figure 6 shows the same effects at 100 feet depth. High frequen-
cies were suppressed and certain frequency components were enhanced.
Note how the component at about 40 cycles per second is increased by
the increasing amounts of excess nitrogen. Also note the component at
70 cycles per second. The frequency of this component is nearly con-
stant but the increasing amounts of nitrogen suppressed it in comparison
to the other frequencies present. A strong 60 cycle per second hum
appears in Figure 6(d) as a very narrow spike illustrating the effects of
a long duration pulse.

At 150 feet depth the frequency enhancing effect of added nitrogen
is dramatic. The two pulses appearing in Figure 7(d) can be identified in

(a) 6.45 liter transducer
Depth 50 feet
H_2 ; 0.67 liter
O_2 ; 0.33 liter

(b) 6.45 liter transducer
Depth 50 feet
H_2 : 0.67 liter
O_2 : 0.33 liter
N_2 : 1.00 liter

(c) 6.45 liter transducer
Depth 50 feet
H_2 : 0.67 liter
O_2 : 0.33 liter
N_2 : 2.00 liter

(d) 6.45 liter transducer
Depth 50 feet
H_2 : 0.67 liter
O_2 : 0.33 liter
N_2 : 3.00 liter
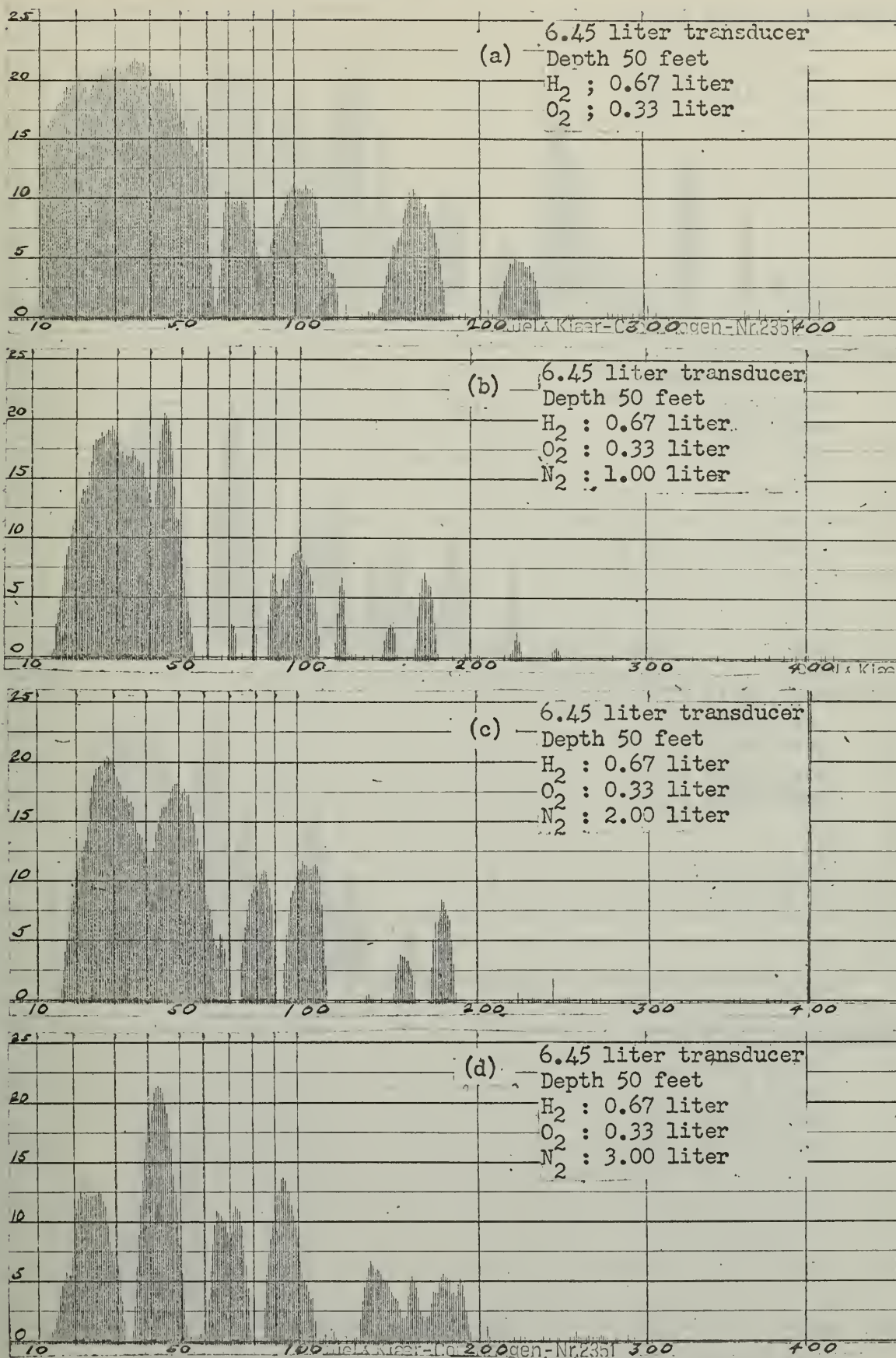
Fig. 5 Spectrum as a Function of Varying Excess N_2, Depth 50 ft.
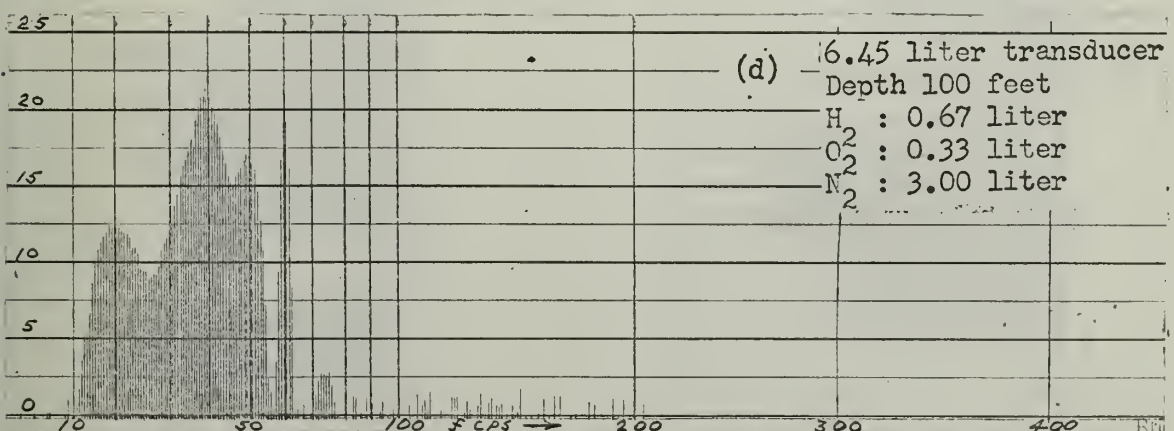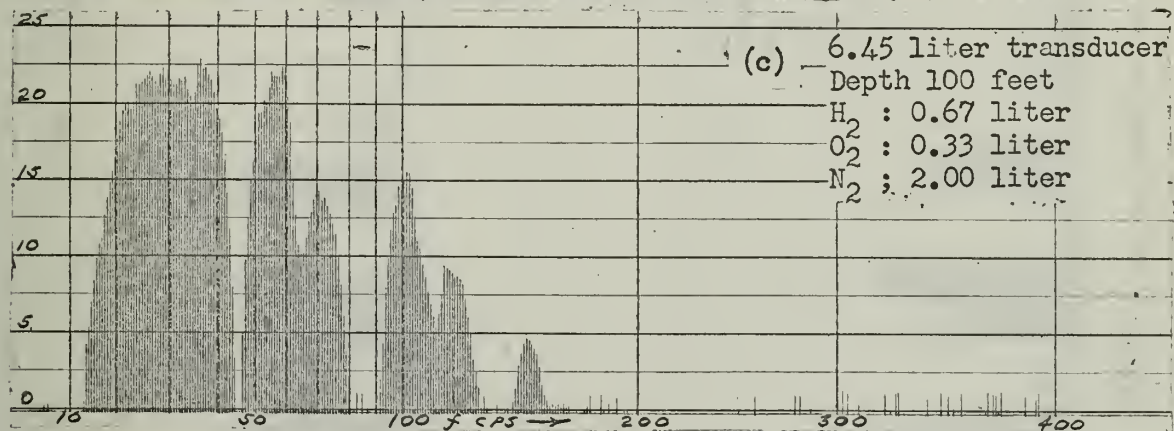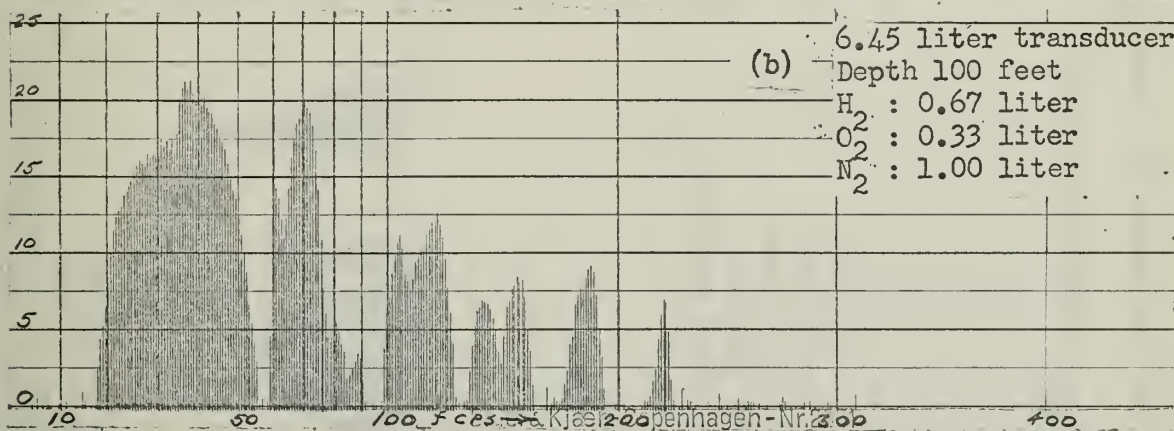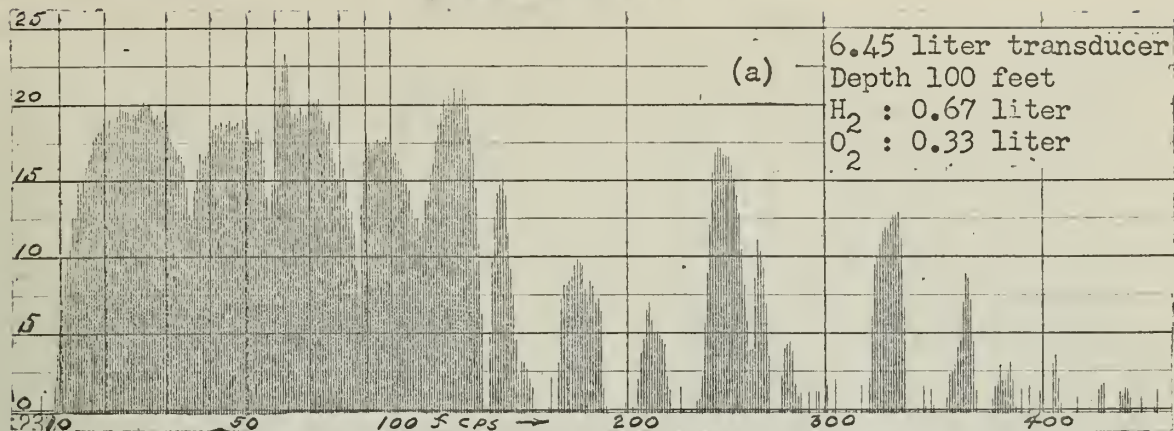
Fig. 6   Spectrum as a Function of Varying Excess N_2, Depth 100 ft.

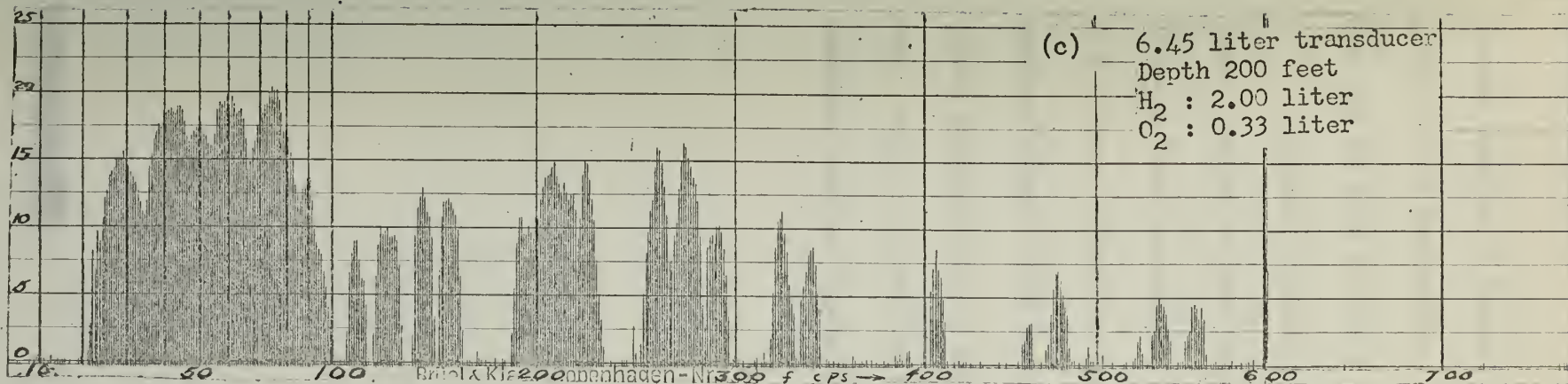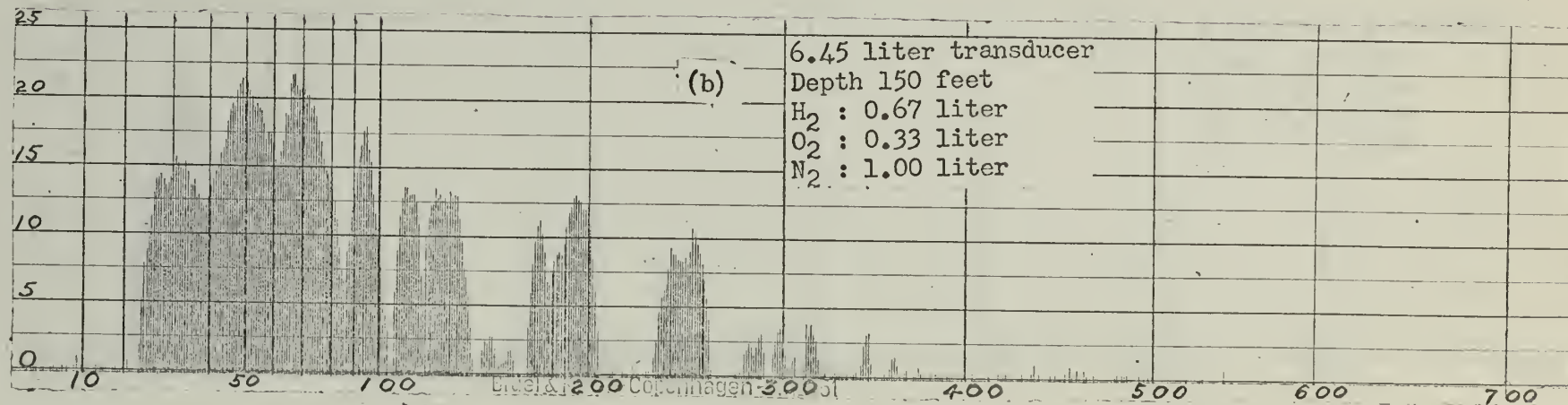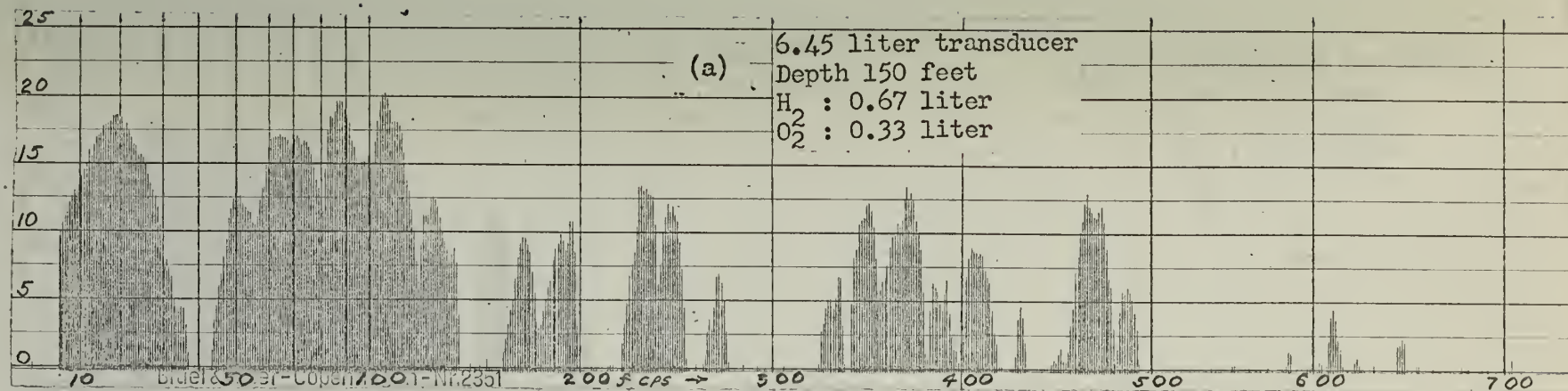Fig. 7 Spectrum as a Function of Varying Excess N_2, Depth 150 ft.

(c) 6.45 liter transducer
Depth 150 feet
H_2 : 0.67 liter
O_2 : 0.33 liter
N_2 : 2.00 liter

(d) 6.45 liter transducer
Depth 150 feet
H_2 : 0.67 liter
O_2 : 0.33 liter
N_2 : 3.00 liter
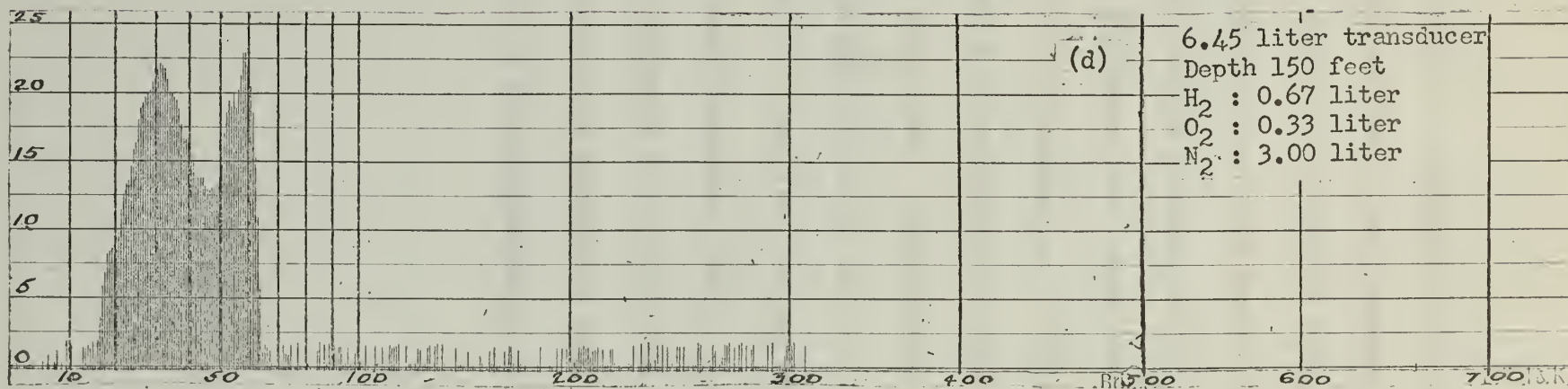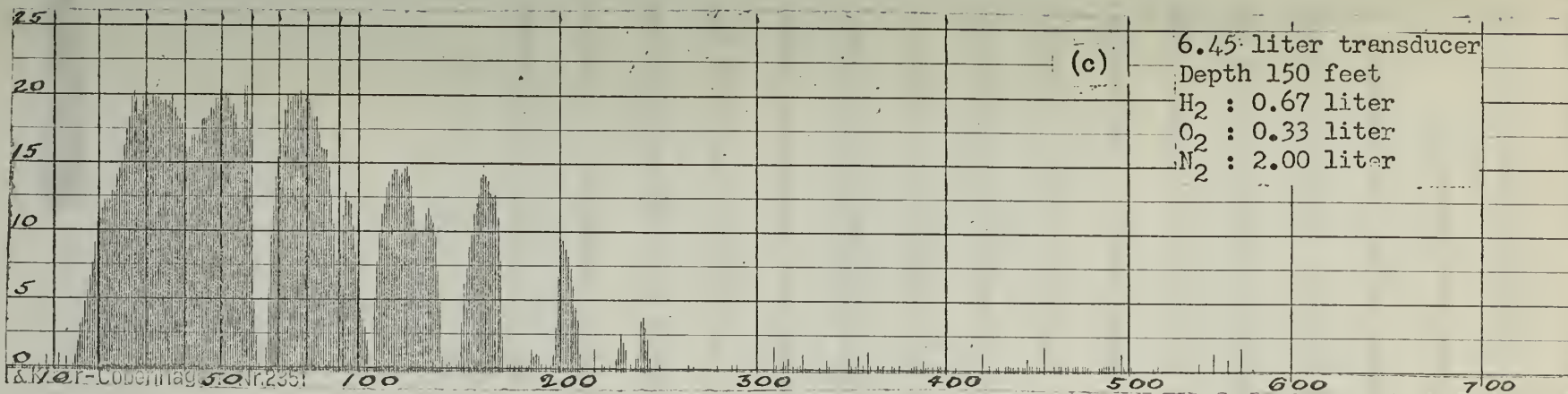
Fig. 7

the other three explosions of Figure 7.

An attempt was made with the explosions displayed in Figure 8 to compare the spectra produced by excess nitrogen to that produced by excess hydrogen. Figures 8(a) and 8(b) differ only in that the former has one liter excess nitrogen while the latter has one liter excess hydrogen. Figures 8(c) and 8(d) have two liters excess nitrogen and hydrogen respectively. There appears to be little difference; the spectra are remarkably alike for nitrogen and hydrogen as the excess gas. Figures 8(e) through 8(h) show the frequency spectra for explosions in which the excess gas volume was increased to three liters. Figure 8(f) produced by the hydrogen excess contains frequencies at 80, 90, and 115 cycles per second that are entirely absent in Figure 8(e). Figure 8(g) and 8(h) have components at nearly the same frequencies, but in the hydrogen rich explosion the higher frequency component is at 115 cycles per second. This upward shift was confirmed by other explosions (not shown) to ensure that it was not the result of some experimental error.
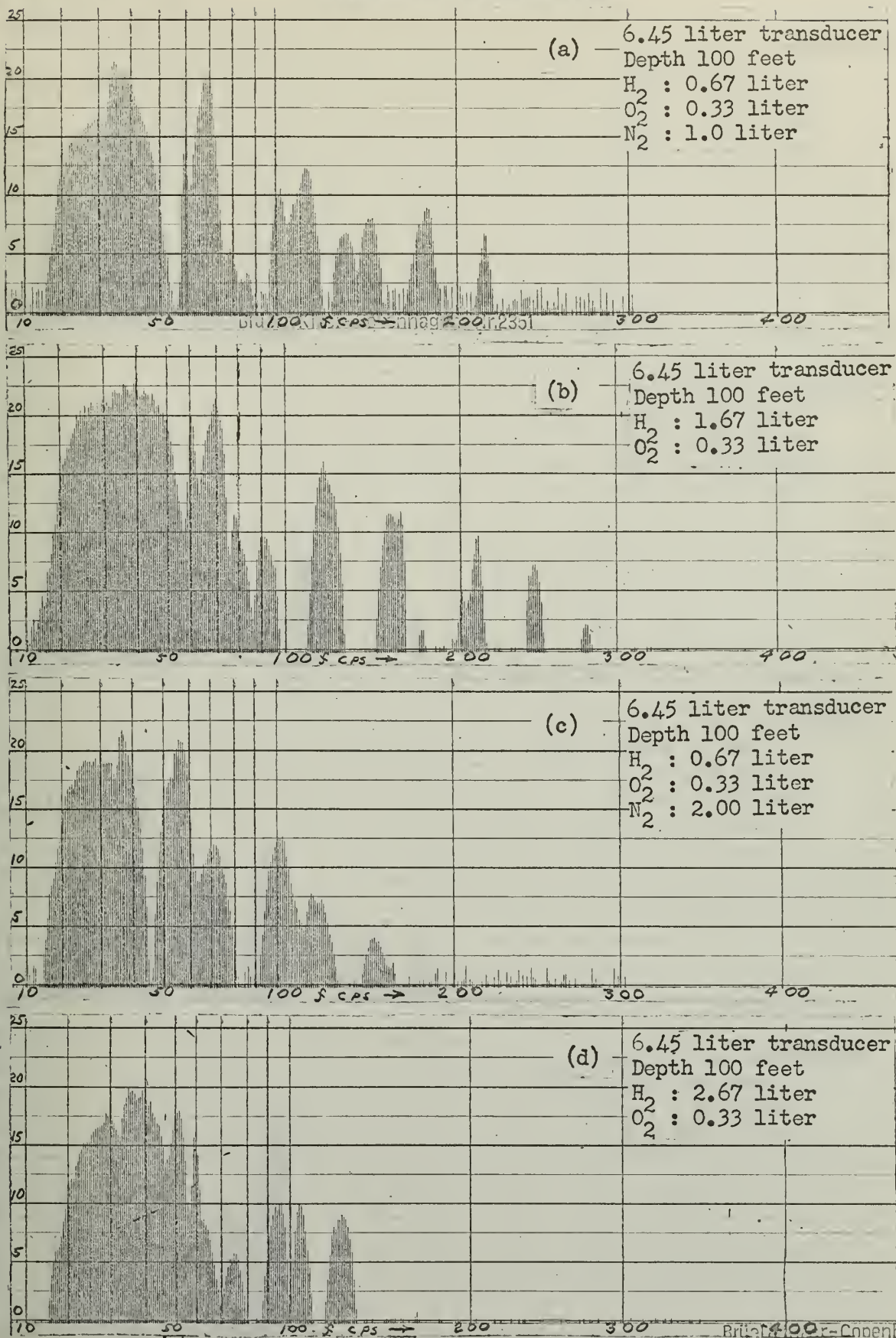
Fig. 8   Comparison of H_2 and N_2 as Excess Gas

20

(e) 6.45 liter transducer
Depth 100 feet
H_2 : 0.67 liter
O_2 : 0.33 liter
N_2 : 3.00 liter

(f) 6.45 liter transducer
Depth 100 feet
H_2 : 3.67 liter
O_2 : 0.33 liter

(g) 6.45 liter transducer
Depth 50 feet
H_2 : 0.67 liter
O_2 : 0.33 liter
N_2 : 3.00 liter

(h) 6.45 liter transducer
Depth 50 feet
H_2 : 3.67 liter
O_2 : 0.33 liter
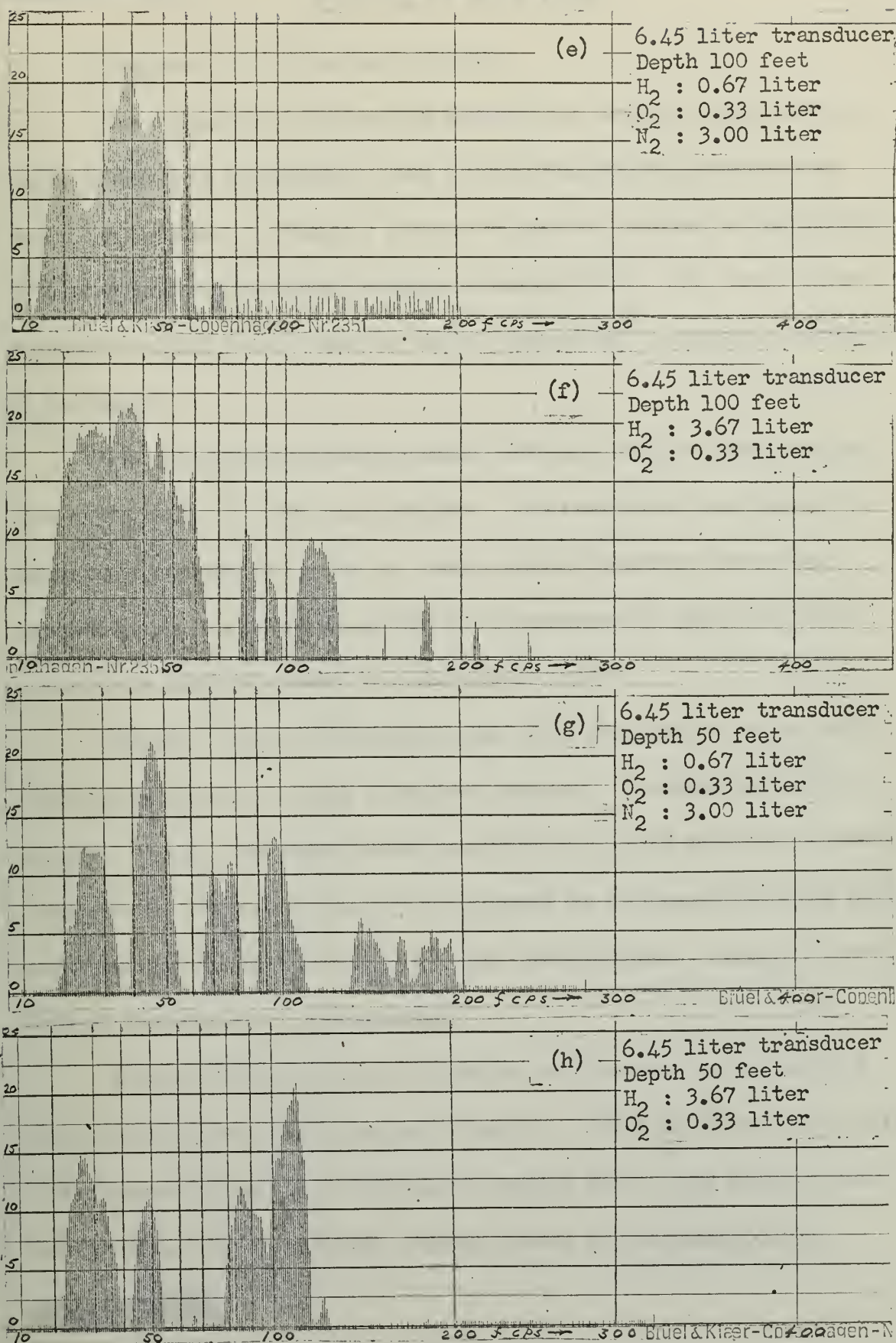
Fig. 8

5.   Frequency as a Function of Depth

The influence of varying the depth of the explosion was investigated in detail in an attempt to find a functional relationship between depth and frequency. Figure 9 shows the spectra produced by explosions of one liter of stoichiometric mixture at depths of 50, 100, and 150 feet. A marked shift of energy into the higher frequencies is evident when depth is increased.

The same stoichiometric mixture with one liter of added nitrogen was exploded at 50, 100, and 150 feet. The spectra for this series of explosions appears in Figure 10. Again higher frequency components appear, but it is also apparent that the frequencies of the strong components are shifting upward with increasing depth.

Figure 11 shows the effect of the same sequence of depths on a charge containing two liters of excess nitrogen. The same tendency is evident, that is, increased depth results in an upward shift of the strong components. Figure 12 displays the spectra for a charge with three liters extra nitrogen at depths of 50, 100, 150, and 200 feet. Here the upward shift of frequencies is unmistakable.

Similar runs with excess hydrogen verified that the same trend would be produced as with excess nitrogen. Figure 13 shows the spectra of explosions using 4 to 1 hydrogen to oxygen ratio. The spectrum was broadened and the frequencies shifted upward by increasing depth

UNCLASSIFIED

(a)   6.45 liter transducer
Depth 50 feet
H_2 : 0.67 liter
O_2 : 0.33 liter

Brüel-Cobenhac 200 (235)

f CPS →

(b)   6.45 liter transducer
Depth 100 feet
H_2 : 0.67 liter
O_2 : 0.33 liter

Brüel & Kjær-Copenhags 200 233

f CPS →
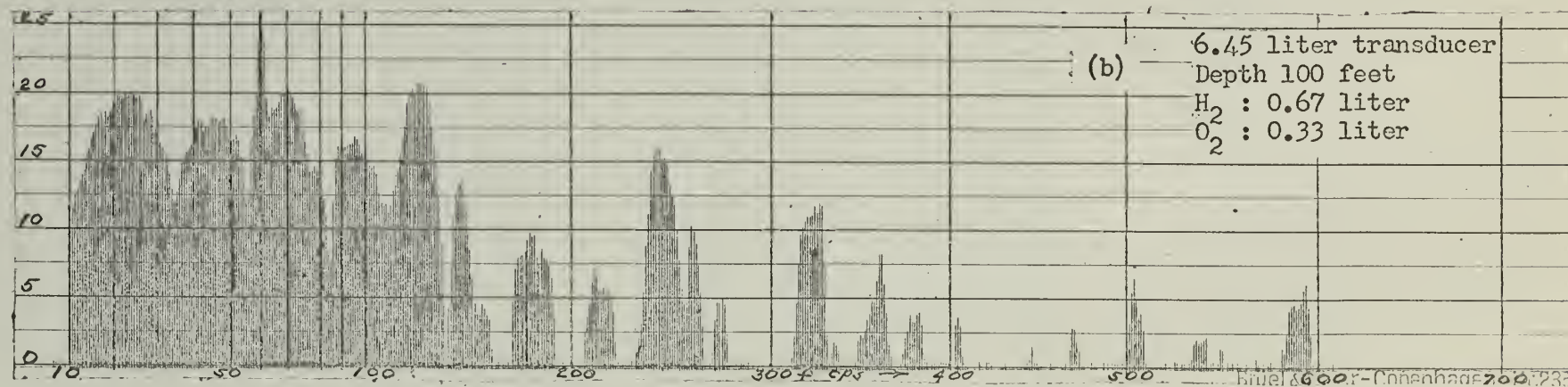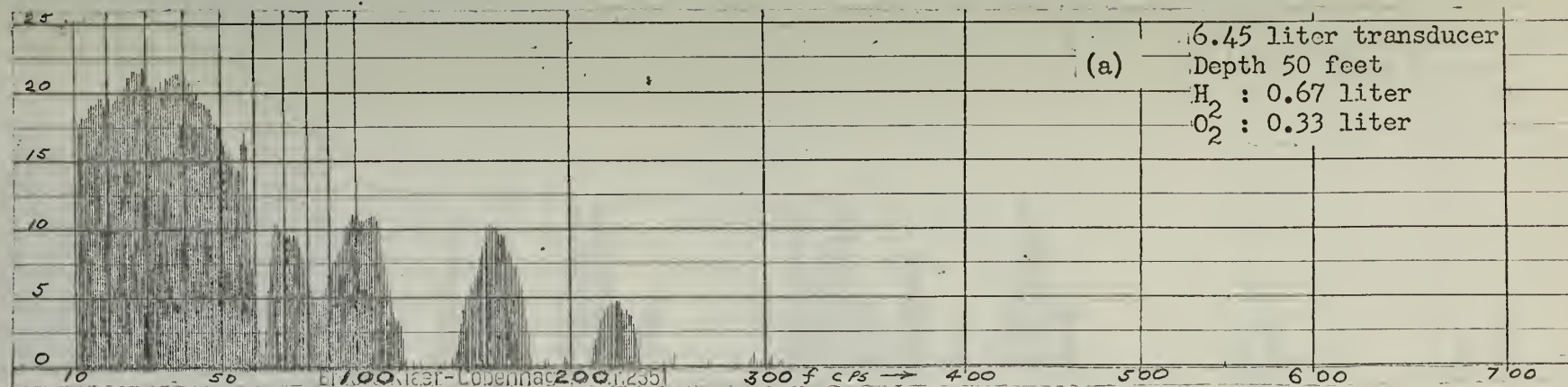
Fig. 9 Spectrum as a Function of Depth, No Excess Gas

Fig. 9

24
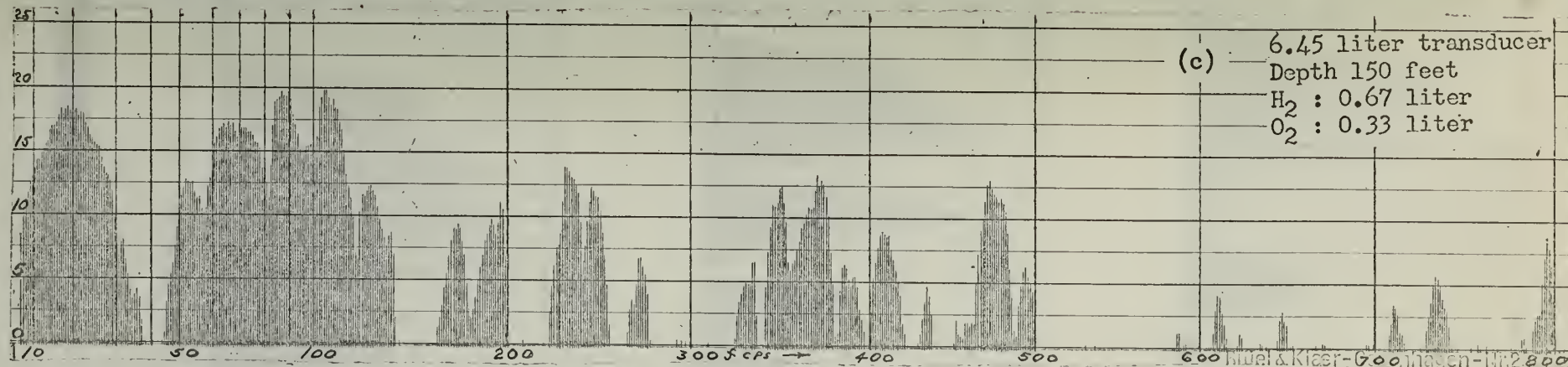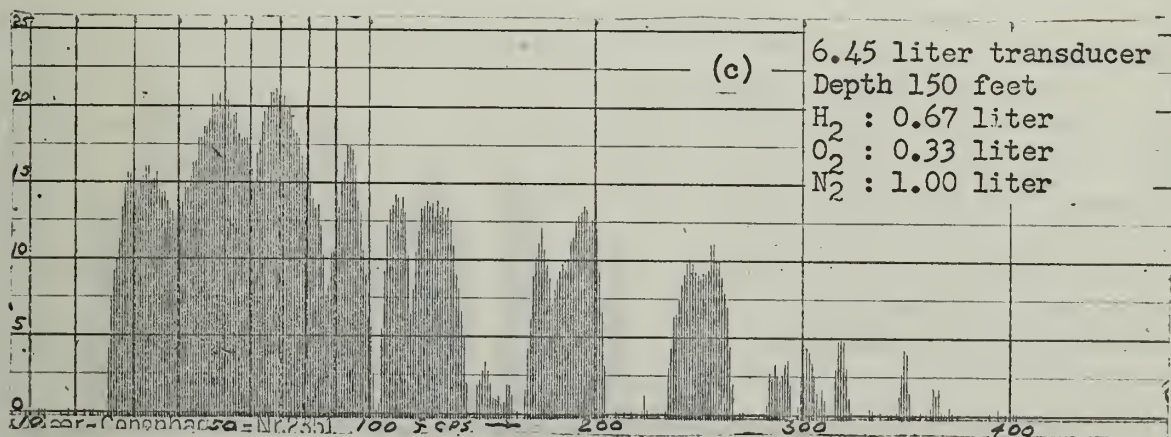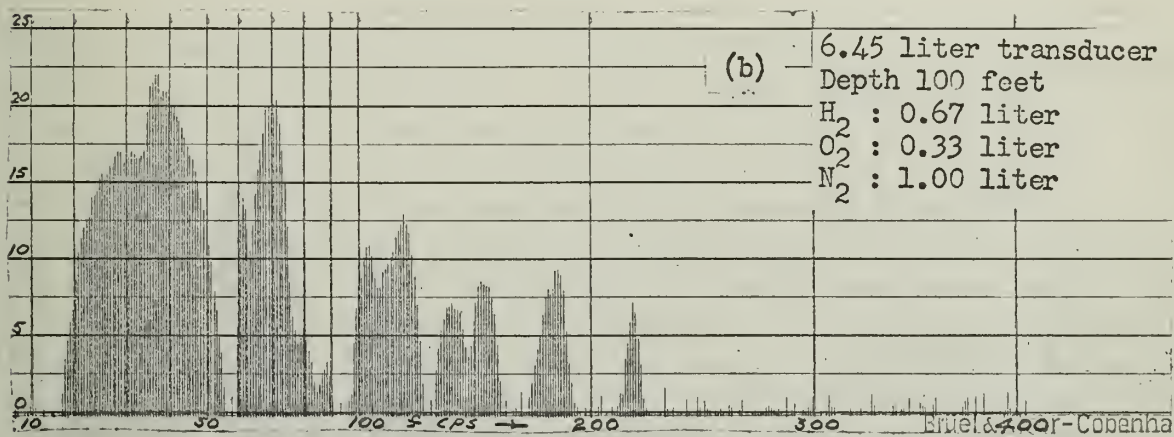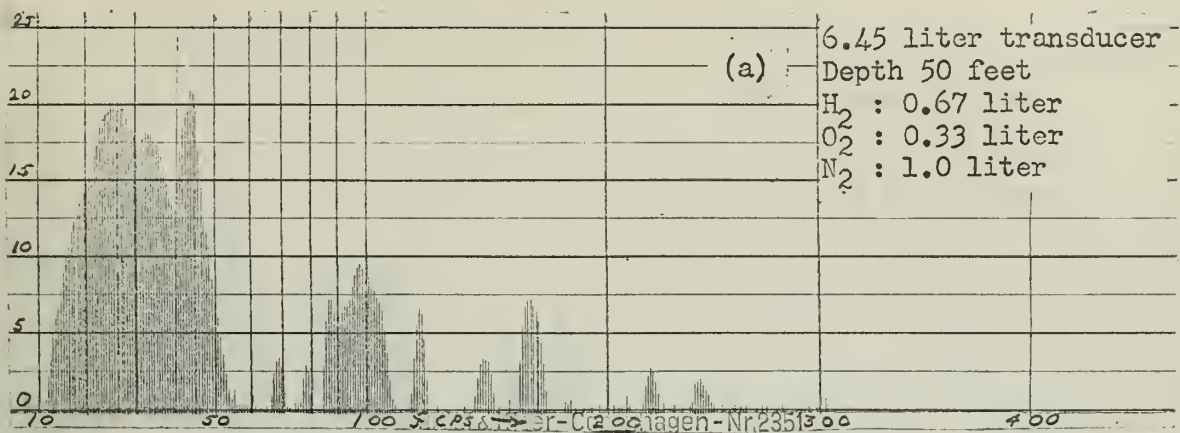
Fig. 10   Spectrum as a Function of Depth, 1.0 liter Excess N_2
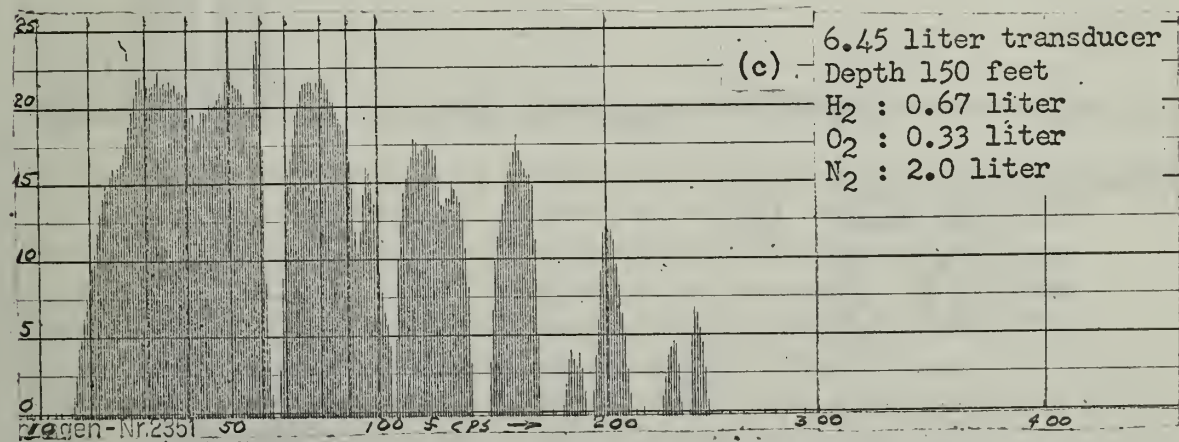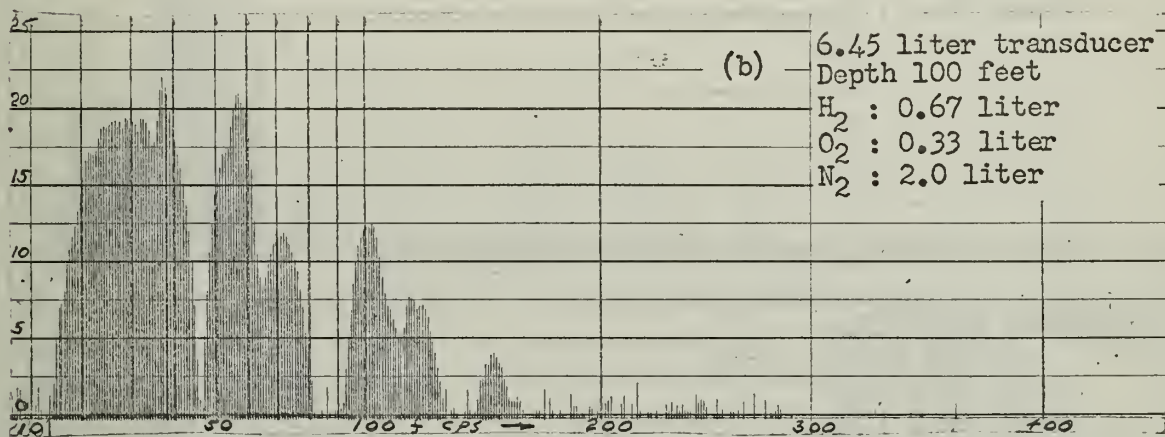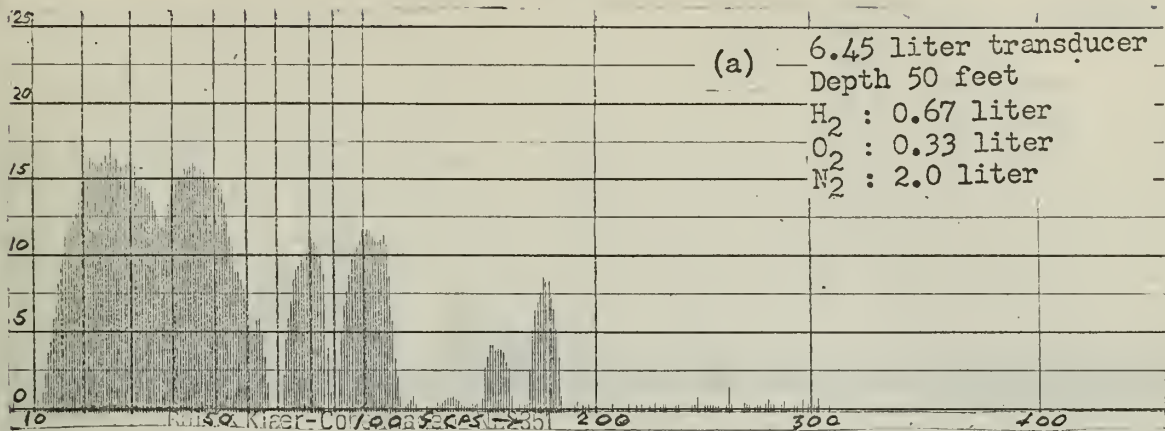
Fig. 11   Spectrum as a Function of Depth, 2.0 liter Excess N_2

(a) 6.45 liter transducer
Depth 50 feet
H_2 : 0.67 liter
O_2 : 0.33 liter
N_2 : 3.00 liter

(b) 6.45 liter transducer
Depth 100 feet
H_2 : 0.67 liter
O_2 : 0.33 liter
N_2 : 3.00 liter

(c) 6.45 liter transducer
Depth 150 feet
H_2 : 0.67 liter
O_2 : 0.33 liter
N_2 : 3.00 liter

(d) 6.45 liter transducer
Depth 200 feet
H_2 : 0.67 liter
O_2 : 0.33 liter
N_2 : 3.00 liter
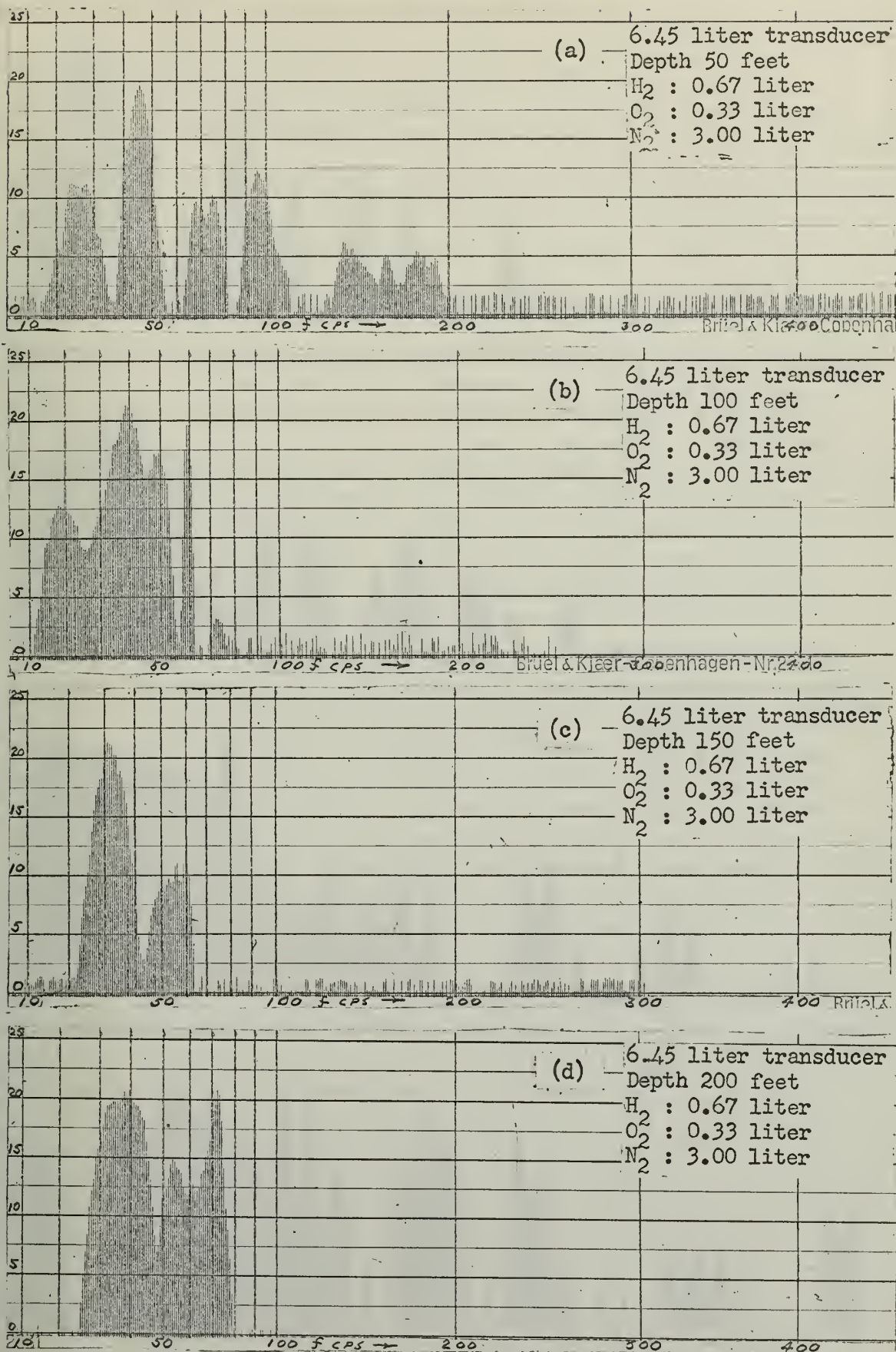
Fig. 12 Spectrum as a Function of Depth, 3.0 liter Excess N_2
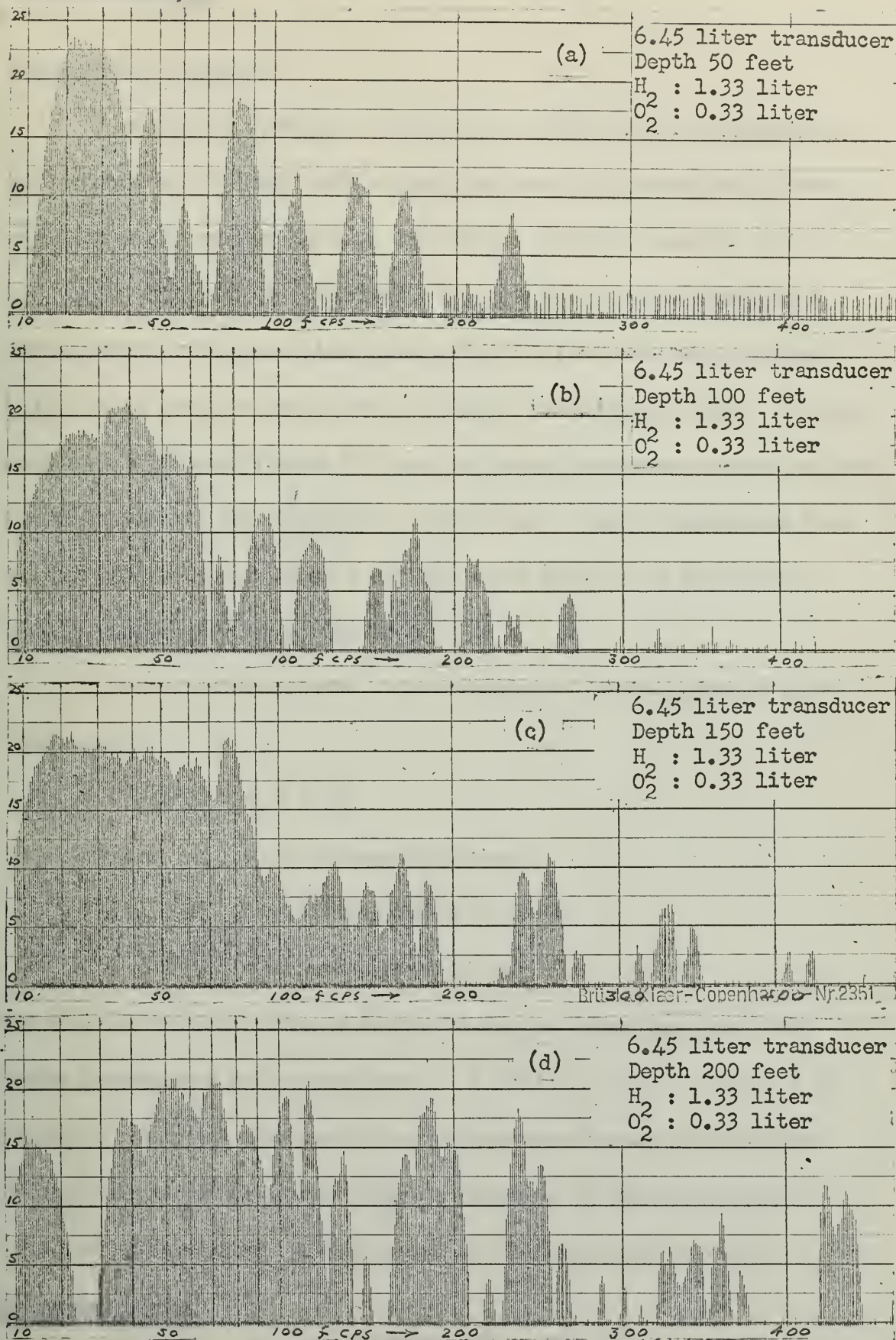
Fig. 13 Spectrum as a Function of Depth, 0.67 liter Excess H_2

CONFIDENTIAL

(Hydrostatic Pressure).

A mixture of hydrogen, oxygen, and nitrogen in the proportions corresponding to a chemically correct mixture of hydrogen and air was exploded at increasing depths. The depths selected were 25, 50, 75, 100, 125, 150, 175, and 200 feet. The spectra of these explosions are exhibited in Figures 14(a) through 14(h). The time based pictures of the sound pressure are shown in Figures 15(a) through 15(h). In the frequency spectra of Figure 14 there are three components which can be traced throughout the sequence of explosions. These frequencies have been plotted in Figure 16 on a log-log scale against the hydrostatic pressure corresponding to the depth.

The slope of the three lines corresponds to the exponent in the relationship:

$$f_o = K \; P_o^n$$

where f_o = the resonant frequency

        K = a proportionality constant

        P_o = hydrostatic pressure

The slopes from the curves of Figure 16 for the lower, medium, and higher frequencies are respectively, $n = 1.14$, $n = 1.01$, and $n = 0.99$. A nearly first power relationship exists between frequency and hydrostatic pressure which agrees with the treatment of the transducer as a Helmholtz Resonator. A discussion of the associated theory in

CONFIDENTIAL

(a)
6.45 liter transducer
Depth 25 feet
H_2 : 0.67 liter
O_2 : 0.33 liter
N_2 : 1.33 liter

(b)
6.45 liter transducer
Depth 50 feet
H_2 : 0.67 liter
O_2 : 0.33 liter
N_2 : 1.33 liter

(c)
6.45 liter transducer
Depth 75 feet
H_2 : 0.67 liter
O_2 : 0.33 liter
N_2 : 1.33 liter

(d)
6.45 liter transducer
Depth 100 feet
H_2 : 0.67 liter
O_2 : 0.33 liter
N_2 : 1.33 liter
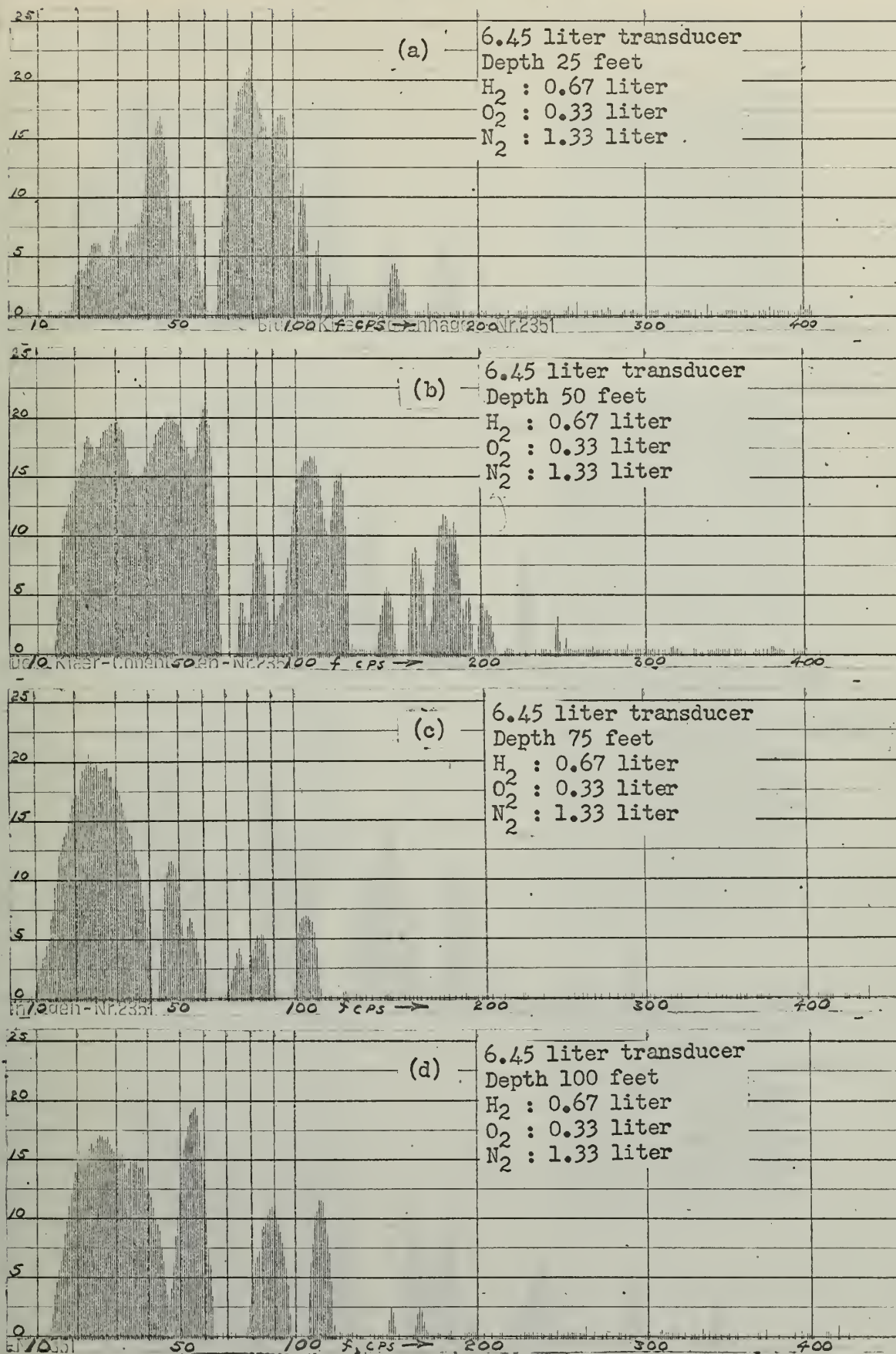
Fig. 14 Spectrum as a Function of Depth, H_2 and Air Mixture

30

(e) — 6.45 liter transducer
Depth 125 feet
H_2 : 0.67 liter
O_2 : 0.33 liter
N_2 : 1.33 liter

(f) — 6.45 liter transducer
Depth 150 feet
H_2 : 0.67 liter
O_2 : 0.33 liter
N_2 : 1.33 liter

(g) — 6.45 liter transducer
Depth 175 feet
H_2 : 0.67 liter
O_2 : 0.33 liter
N_2 : 1.33 liter

(h) — 6.45 liter transducer
Depth 200 feet
H_2 : 0.67 liter
O_2 : 0.33 liter
N_2 : 1.33 liter
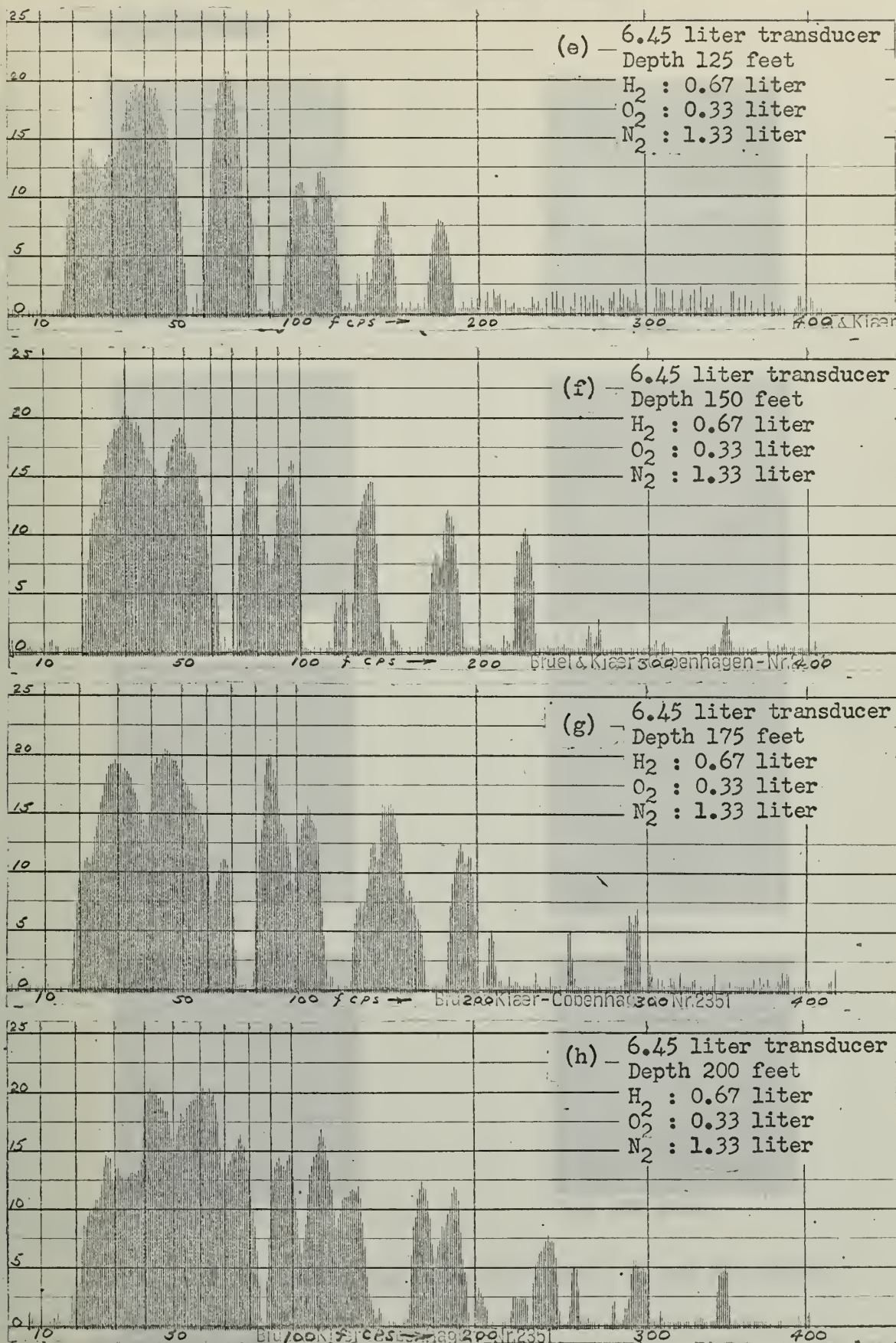
Fig. 14

(a) 25 feet

(b) 50 feet

(c) 75 feet

(d) 100 feet

(e) 125 feet

(f) 150 feet

(g) 175 feet

(h) 200 feet

Fig. 15 Time Domain Variation with Depth, H_2 and Air mixture
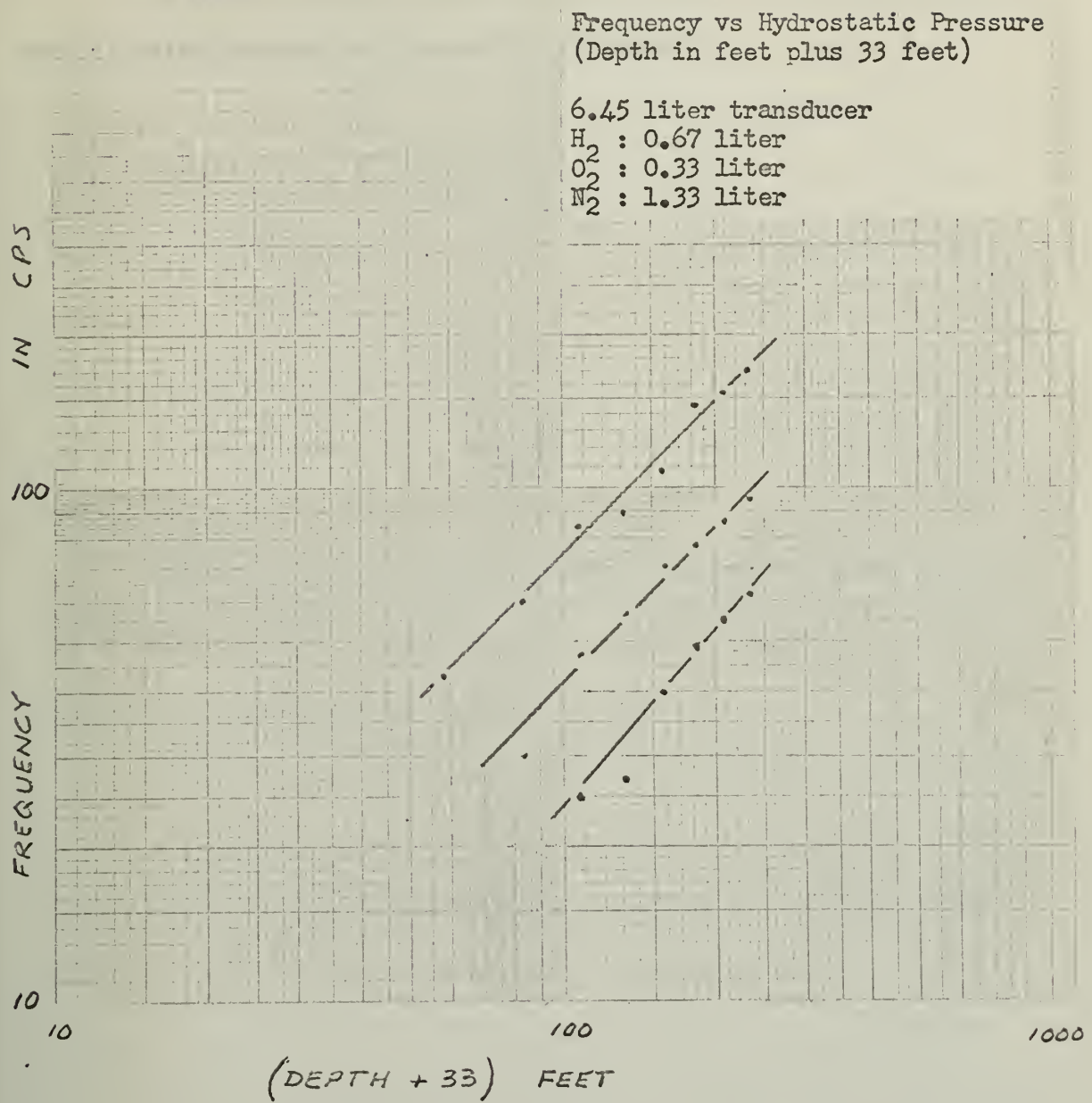
Fig. 16 Frequency vs. Hydrostatic Pressure

Section 9 explains this first power relationship.

The time domain pictures in Figure 15 show the pulse shortening which causes the spectral broadening of Figure 14.

6. Spectral Broadening Due to Surface Reflections

The spectrum of the explosion at 50 feet, Figure 14(b) appears
to be inconsistent with the otherwise observed trends. There are fre-
quencies above 100 cycles per second and frequencies missing in the
vicinity of 90 cycles per second. Referring back to Figure 12(a) there
is another explosion at 50 feet depth which is not in agreement with
expectations. The components between 100 and 200 cycles per second
are the unexpected ones. Again in Figure 11(a) the component at 175
cycles per second does not fit the rule for decreasing frequencies with
reduced depth.

Figure 17(a) is the time picture corresponding to the spectrum of
Figure 12(a). At about 15 milliseconds from the beginning of the pulse
the result of a surface reflection can be seen.

The hydrophone was located 40 feet horizontally from the source
for this recording at a depth of 50 feet so that the direct wave path was
40 feet while the reflected wave path was 108 feet. The path length
difference is 68 feet which produces a time delay of about 14 milli-
seconds. Beginning at 14 milliseconds there was a strong reflected
wave arriving at the hydrophone along with the direct wave. The surface
reflection is a negative reflection and the waveform actually recorded
was a complex resultant of both direct and reflected waves.

(a)

(b)

(c)
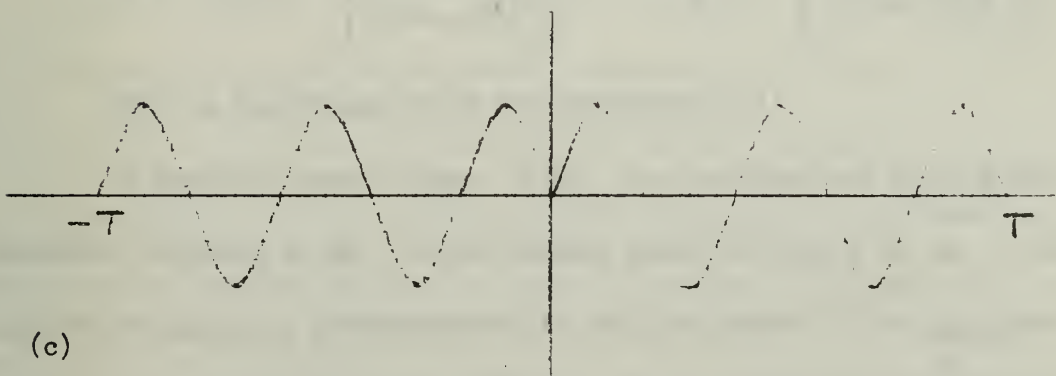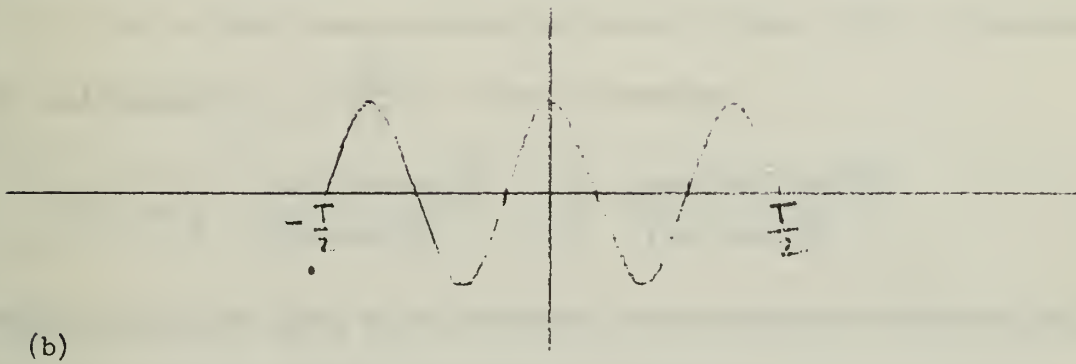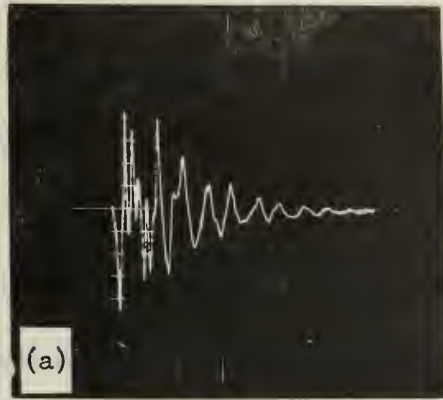
Fig. 17 Surface Reflection Effects

A surface reflection can produce a profound influence on the frequency spectrum of the resultant pressure wave. A superficial approach might lead one to presume that the frequencies present in the direct wave would also be present in the reflected wave so there would be no difference in the frequency domain with or without reflections. The fact is that reflections can cause, under certain conditions, nearly total suppression of frequencies present in the direct wave accompanied by disproportionate boosting of the side bands.

As an ideal case consider the pulse of Figure 17(b), of duration T, and frequency $f_0 = \dfrac{\omega_0}{2\pi}$. It has a spectrum:

$$F(\omega) = \frac{T}{2} \; \frac{\sin(\omega+\omega_0)\frac{T}{2}}{(\omega+\omega_0)\frac{T}{2}} + \frac{T}{2} \; \frac{\sin(\omega-\omega_0)\frac{T}{2}}{(\omega-\omega_0)\frac{T}{2}}$$

Now consider the same pulse followed immediately by a reflected pulse as shown in Figure 17(c). It has the spectrum:

$$F(\omega) = \frac{(\omega+\omega_0)T^2}{2}\left[\frac{\sin(\omega+\omega_0)\frac{T}{2}}{(\omega+\omega_0)\frac{T}{2}}\right]^2 - \frac{(\omega-\omega_0)T^2}{2}\left[\frac{\sin(\omega-\omega_0)\frac{T}{2}}{(\omega-\omega_0)\frac{T}{2}}\right]^2$$

(For an analytical proof see Appendix IV.)

In the first case, Figure 17(b), the spectrum has a $\underline{\dfrac{\sin x}{x}}$ distribution centered at ω_0. In the second case the output at ω_0 is zero and the frequencies corresponding to the side bands of the $\underline{\dfrac{\sin x}{x}}$ distribution are boosted by 5.5 decibels. The condition which produces

this phenomenon is a phase shift of π radians of the fundamental

frequency.

Now consider one cycle of period 14 milliseconds followed

immediately by a negative reflection of itself delayed 14 milliseconds.

This satisfies the phase relationship. Refer to Figure 12(a) and ob-

serve that the 14 millisecond period corresponds to 72 cycles per

second. If the duration is 14 milliseconds the first side band of the

$\underline{\sin x}$ distribution will be at 180 cycles per secondand and it will be
x

enhanced.

The same sort of reasoning can be applied to the explosion at

50 feet shown in Figures 14(b) and 15(b). The period of the first cycle

is about 13 milliseconds corresponding to a frequency of 77 cycles per

second. At 180 cycles per second there is the raised sideband where

$x = \dfrac{3}{2}\pi$, and at 140 cycles per second there is a minimum where

$x = \pi$ in the $\underline{\sin x}$ distribution.
$\phantom{x = \pi \text{ in the }}x$

Of course the spectra of Figures 17(b) and 17(c) are ideal and

have been used only because they are mathematically convenient.

However the idea that strong surface reflections can distort the fre-

quency spectrum is an important consideration and considerable modi-

fication of the measurements at depths less than 100 feet exists.

7.   Effect of Different Transducers

Throughout the discussions of the preceding sections the explosions considered were all set off in the 6.45 liter transducer. In order to obtain some idea of the influence of transducer size and shape on the acoustic spectrum, explosions were set off in three other transducers. The 7.30 liter transducer is the one used by Harris and Rigsbee and referred to in their work as the "basic transducer". The 22.8 liter transducer was a design used in later work by the same authors. These two transducers are similar in geometry to the 6.45 liter transducer; all three are cylindrical in shape but differ in size. Data for the transducers is furnished in Appendix III. The 7.30 liter transducer has a hemispherically shaped top while the other transducers have flat tops. A comparison of the frequency spectra for these three transducers is made in Figure 18. The characteristics of the spectra are similar but the frequencies are shifted by the transducer geometry.

The 4.03 liter transducer used in the experiments of Figure 19 was quite different in shape. It was six feet long and only two inches in diameter. Consider Figure 19(a) for the stoichiometric mixture. The spectral spikes extended all the way out to 2500 cycles per second, the limit of the spectrum analyzer. In Figure 19(b) the mixture was changed to a four to one hydrogen to oxygen ratio. The change produced in the spectrum was dramatic. The charge of figure 19(c) is a five to one

(a) — 7.30 liter transducer
Depth 50 feet
H_2 : 0.65 liter
O_2 : 1.06 liter

(b) — 22.8 liter transducer
Depth 50 feet
H_2 : 0.65 liter
O_2 : 1.06 liter

(c) — 6.45 liter transducer
Depth 50 feet
H_2 : 0.65 liter
O_2 : 1.06 liter
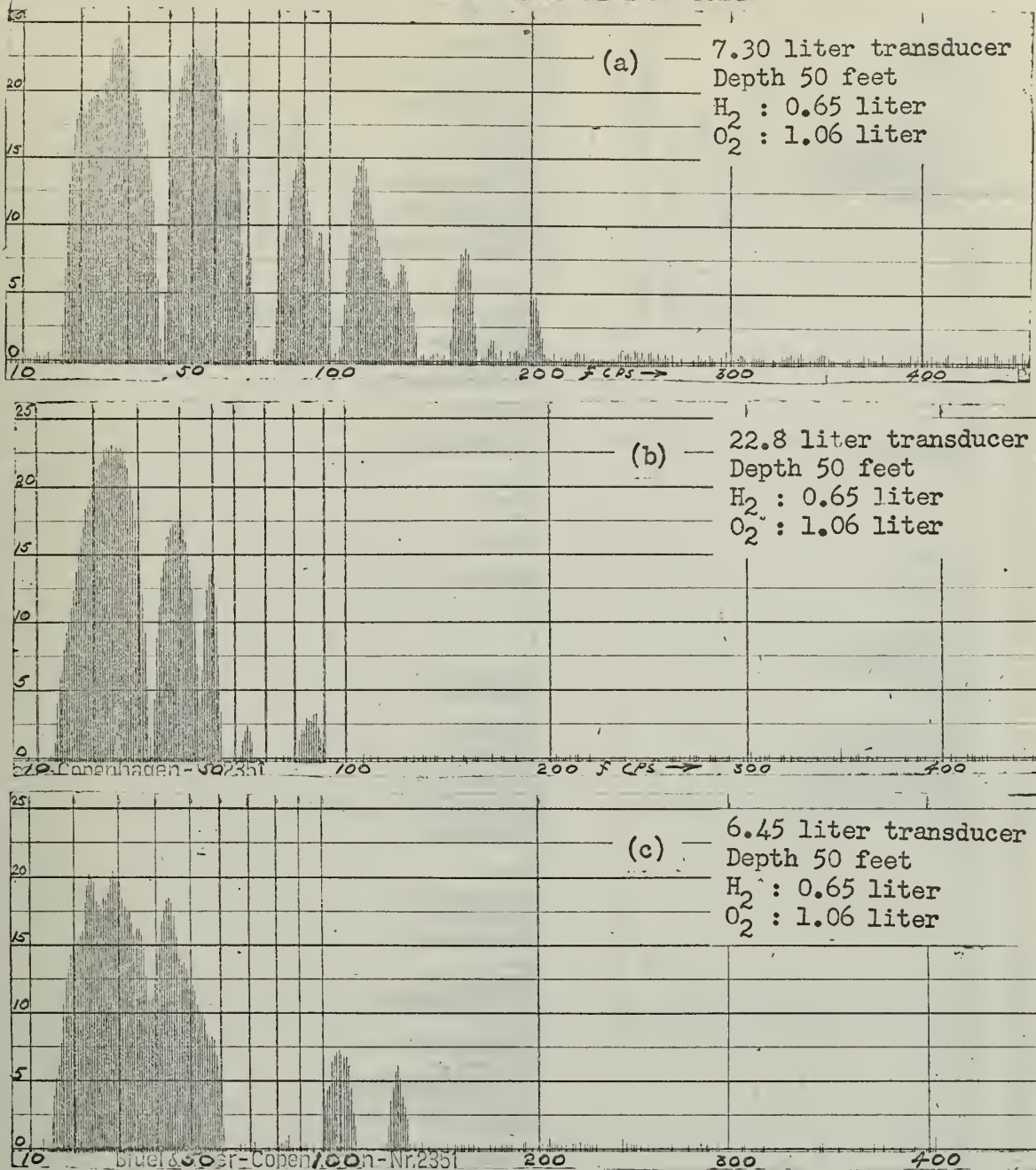
Fig. 18 Spectra Produced by Different Transducers
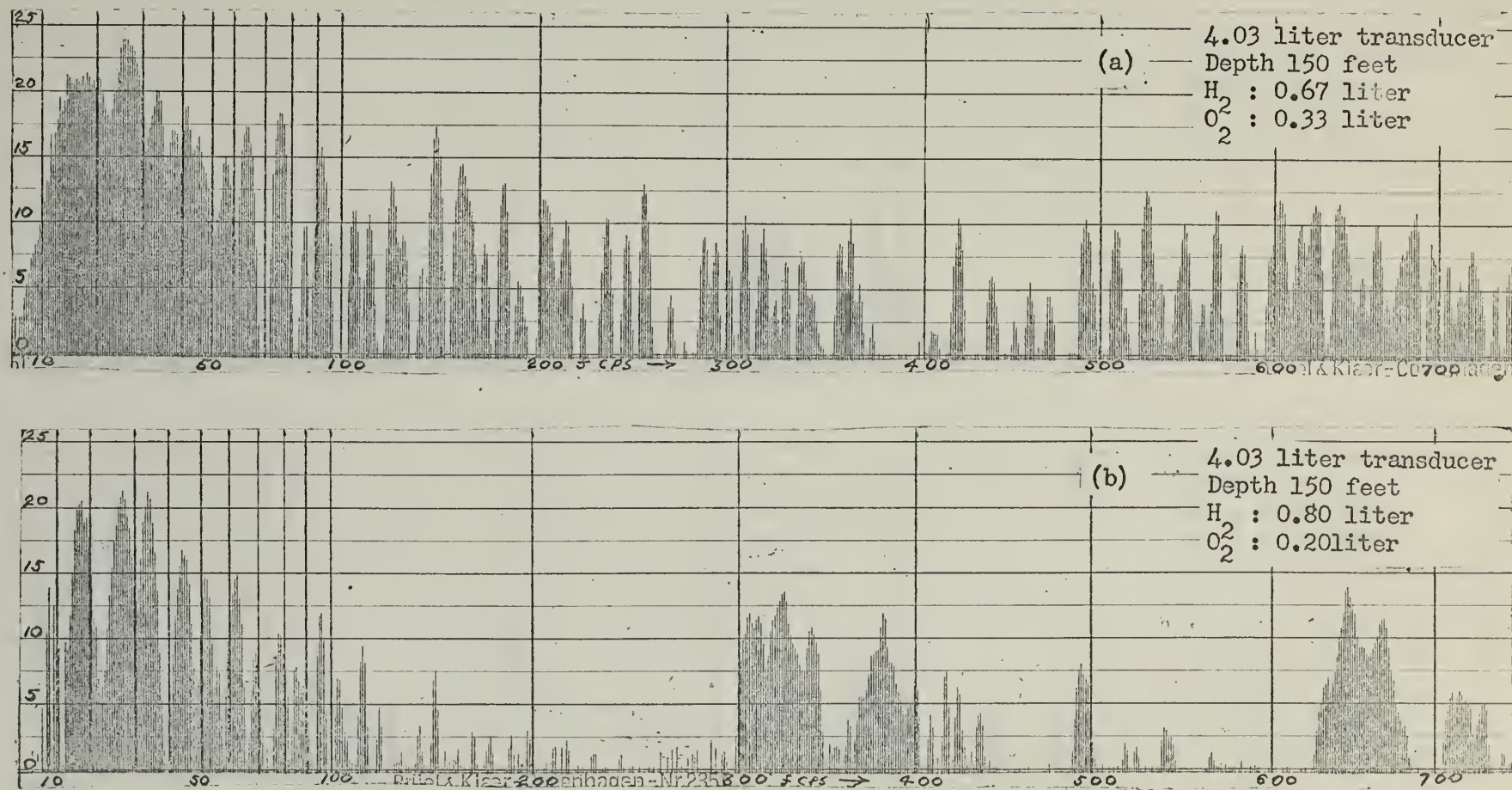
Fig. 19 Spectra Produced by Explosions in Long Narrow Transducer

4.03 liter transducer
Depth 150 feet
H_2 : 0.83 liter
O_2 : 0.17 liter

(c)

4.03 liter transducer
Depth 150 feet
H_2 : 0.86 liter
O_2 : 0.14 liter

(d)

Fig. 19

(e) — 4.03 liter transducer
Depth 150 feet
H_2 : 0.89 liter
O_2 : 0.11 liter

(f) — 4.03 liter transducer
Depth 150 feet
H_2 : 0.50 liter
O_2 : 0.50 liter

Fig. 19

44

(g)   4.03 liter transducer
Depth 150 feet
H_2 : 0.33 liter
O_2^2 : 0.67 liter

(h)   4.03 liter transducer
Depth 150 feet
H_2 : 0.40 liter
O_2^2 : 1.60 liter
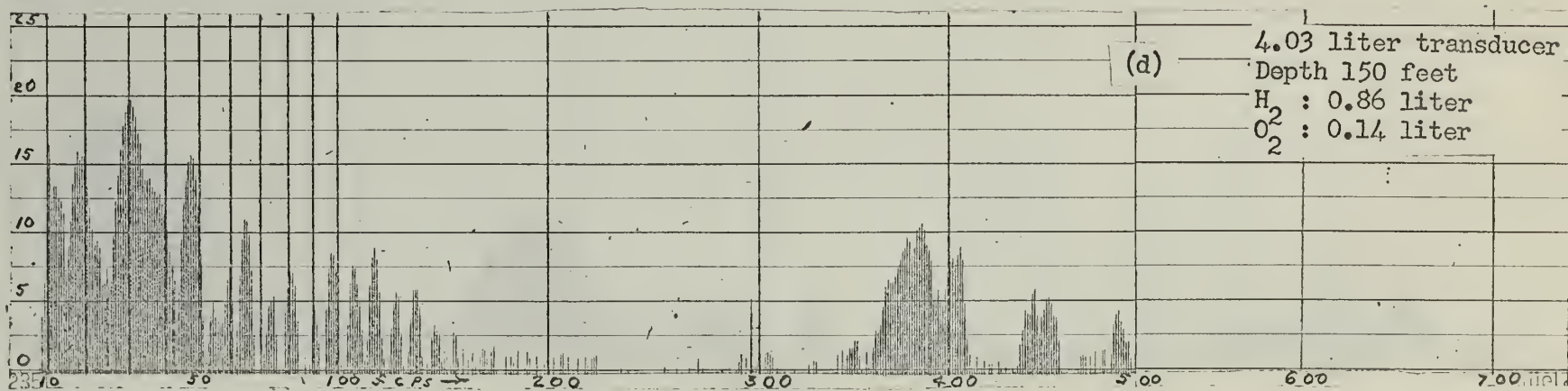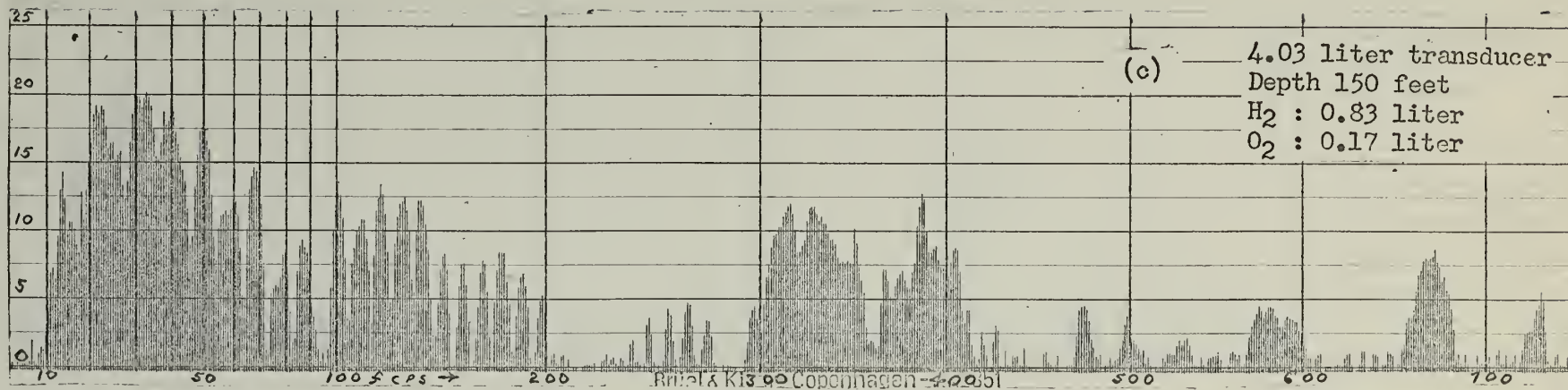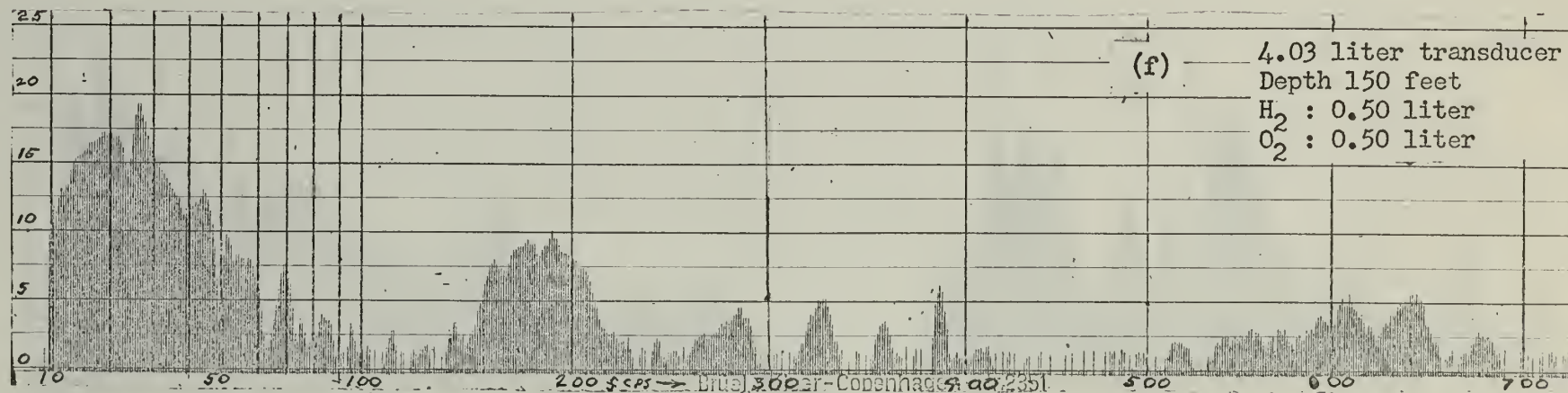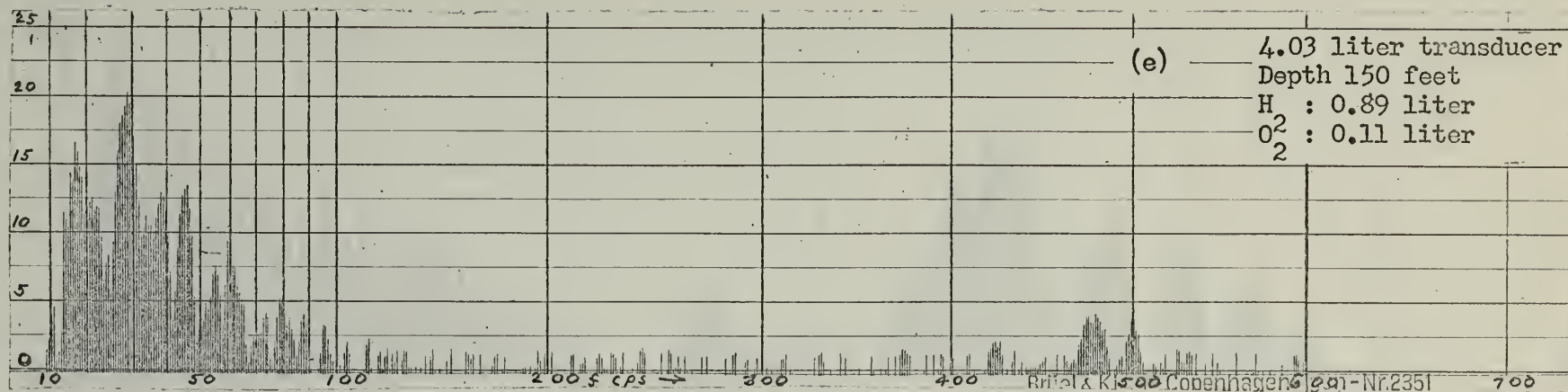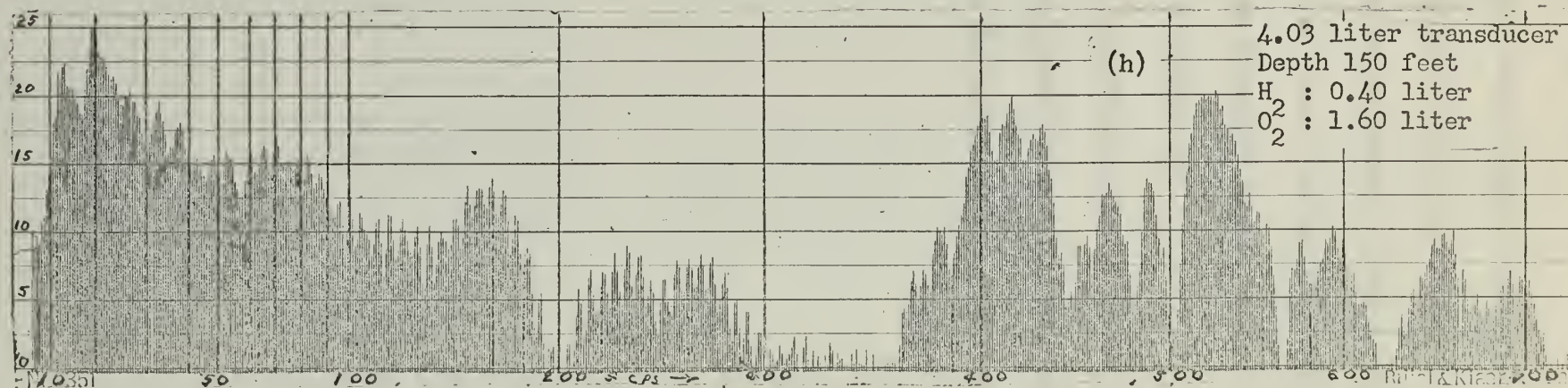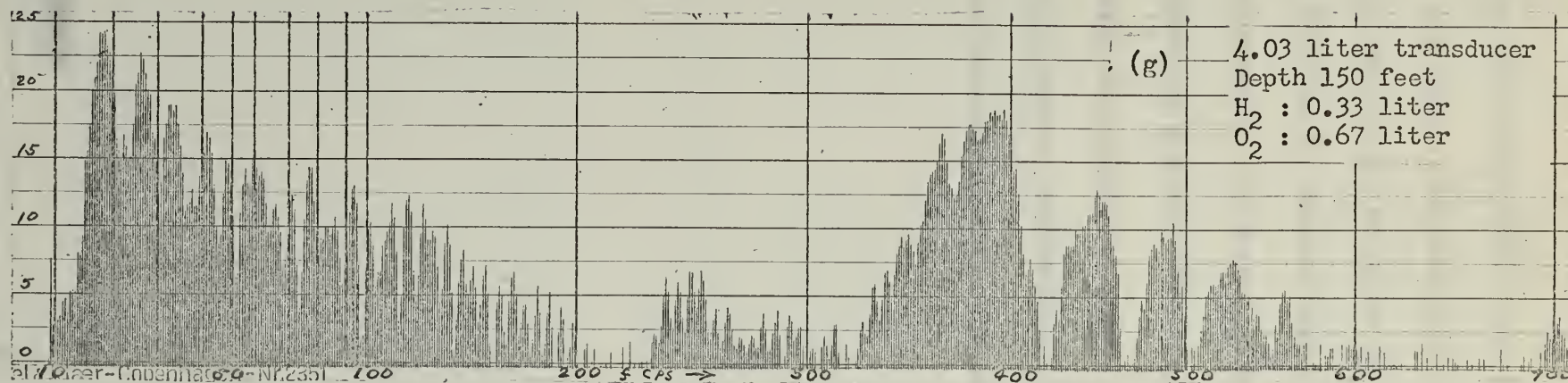
Fig. 19

mixture ratio, and Figure 19(d) is six to one, while Figure 19(e) is for

an eight to one ratio. The noteworthy component here is the persistent

component in the vicinity of 400 to 500 cycles per second. Figures 19(f),

19(g), and 19(h) are for mixture ratios of one to one, one to two, and one

to four respectively. This means an excess of oxygen gas in the com-

bustion chamber for the last three spectra of Figure 19.

Clearly the addition of excess gas has the effect of producing an

enhancement of certain frequencies. Clearly also the configuration of

the container has a strong influence on the output frequency spectrum.

8.   Frequency Shift Phenomenon

The time domain of nearly every acoustic pulse showed an initial frequency of oscillation followed by an abrupt change to a slightly higher frequency. The time pictures have a scale of 20 milliseconds per division except for figures 20(l), 20(m), 20(n), 20(o), the explosions in the 4.03 liter pipe, which have a time scale of 10 milliseconds per division. Where an initial and a final frequency can be distinguished from the time picture, the period has been measured and the frequencies have been computed. Reference has been made to the spectral analysis pictures and these initial and final frequencies have been identified on the spectra. The frequencies measured on the spectral pictures are more accurate. Frequencies from the two sources are tabulated in Table 1 for comparison.

This upward frequency shift appears to be a universal pheno-menon observed throughout the data. One result of it is that the spectrum of each explosion is broadened. The fact that the frequency shift is abrupt and not a frequency slide can be seen from the spectral plots: There are two separate spikes in the frequency domain. The duration of the initial frequency is less than that of the final frequency. This can be seen directly in the time domain, and it may be observed in the frequency domain that the component corresponding to the longer final frequency is narrower than the shorter initial frequency component.

Of most of the time pictures it can be said that the frequency

(a) 6.45 l. transd.
    Depth 100 feet
    H_2 : 2.00 liter
    O_2 : 0.33 liter

(b) 6.45 l. transd.
    Depth 100 feet
    H_2 : 2.67 liter
    O_2 : 0.33 liter

(c) 6.45 l. transd.
    Depth 150 feet
    H_2 : 2.67 liter
    O_2 : 0.33 liter

(d) 6.45 l. transd.
    Depth 50 feet
    H_2 : 0.67 liter
    O_2 : 0.33 liter
    N_2 : 1.00 liter

(e) 6.45 l. transd.
    Depth 50 feet
    H_2 : 0.67 liter
    O_2 : 0.33 liter
    N_2 : 2.00 liter

(f) 6.45 l. transd.
    Depth 100 feet
    H_2 : 0.67 liter
    O_2 : 0.33 liter
    N_2 : 1.00 liter

(g) 6.45 l. transd.
    Depth 100 feet
    H_2 : 0.67 liter
    O_2 : 0.33 liter
    N_2 : 2.00 liter
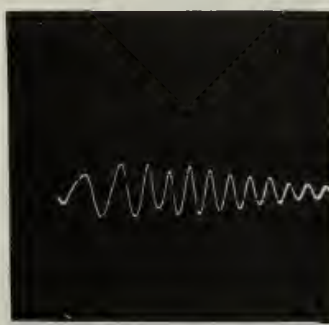
(h) 6.45 l. transd.
    Depth 150 feet
    H_2 : 0.67 liter
    O_2 : 0.33 liter
    N_2 : 3.00 liter
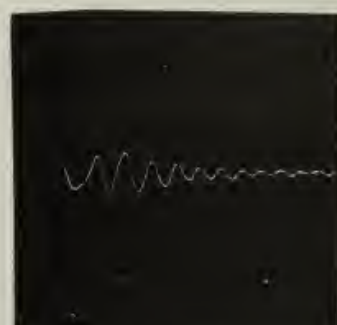
(i) 6.45 l. transd.
    Depth 100 feet
    H_2 : 0.67 liter
    O_2 : 0.33 liter
    N_2 : 3.00 liter

Fig. 20 Frequency Shift in Time Domain

(j) 6.45 l. transd.
Depth 150 feet
H_2 : 0.67 liter
O_2 : 0.33 liter
N_2 : 3.00 liter
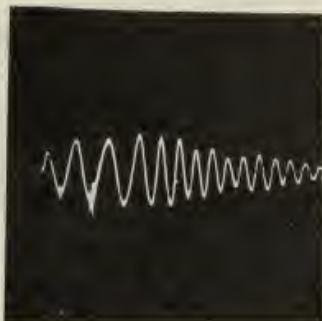
(k) 6.45 l. transd.
Depth 200 feet
H_2 : 0.67 liter
O_2 : 0.33 liter
N_2 : 3.00 liter

(l) 4.03 l. transd.
Depth 150 feet
H_2 : 0.80 liter
O_2 : 0.20 liter

(m) 4.03 l. transd.
Depth 150 feet
H_2 : 0.86 liter
O_2 : 0.14 liter

(n) 4.03 l. transd.
Depth 150 feet
H_2 : 0.33 liter
O_2 : 0.67 liter

(o) 4.03 l. transd.
Depth 150 feet
H_2 : 0.40 liter
O_2 : 1.60 liter

(p) 6.45 l. transd.
Depth 100 feet
H_2 : 1.67 liter
O_2 : 0.33 liter

(q) 6.45 l. transd.
Depth 100 feet
H_2 : 3.67 liter
O_2 : 0.33 liter
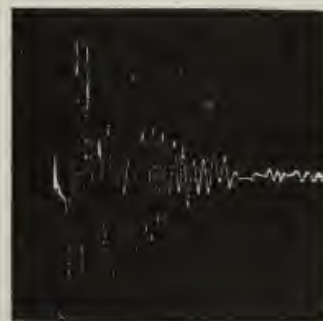
(r) 6.45 l. transd.
Depth 50 feet
H_2 : 3.67 liter
O_2 : 0.33 liter

Fig. 20

shift occurs just following the maximum pressure amplitude. This would seem to indicate that during the time of the initial frequency, burning of the gases is still taking place. The frequency shift may correspond to the end of the actual release of chemical energy.

CONFIDENTIAL

Table 1

Time Base Figure 20	Initial Frequency	Final Frequency	Frequency Spectrum	Initial Frequency	Final Frequency
a	33	62	2(c)	38	62
b	33	50	2(d)	36	56
c	37	67	3(d)	42	68
d	33	45	5(b)	28	45
e	31	53	5(c)	28	50
f	33	70	6(b)	37	70
g	40	55	6(c)	38	57
h	33	58	7(d)	32	58
i	34	50	6(d)	38	48
j	33	62	12(c)	32	56
k	35	75	12(d)	38	73
l	330	500	19(b)	330	490
m	400	475	19(d)	385	450
n	400	510	19(g)	400	
o	400	500	19(h)	410	520
p	38	67	8(b)	38	70
q	36	45	8(f)	36	45
r	56	118	1(a)	49	115

CONFIDENTIAL

9.   Helmholtz Resonator Calculations.

The resonant frequency of the transducer as a Helmholtz Resonator can be calculated by finding the frequency at which the reactance due to the acoustic inertance of the plug of water in the bottom of the transducer equals the reactance due to the acoustic compliance of the volume of gas in the transducer.[1]

V	=	Total volume of transducer.
V_g	=	Volume of gas at firing depth.
V_{og}	=	Volume of gas at one atmosphere.
V_w	=	Volume of water plug.
S	=	Surface area of the end of the container.
a	=	Radius of the cylinder.
ρ_w	=	Density of the sea water.
ρ_g	=	Density of gas at firing depth.
ρ_{og}	=	Density of gas at one atmosphere.
c_g	=	Velocity of sound in the gas.
P	=	Pressure of water at firing depth.
P_o	=	Pressure of one atmosphere.

The acoustic inertance is:

$$M = \frac{\text{mass of water}}{S^2} = \frac{\rho_w V_w}{S^2}$$

[1]L. E. Kinsler and A. R. Frey, Fundamentals of Acoustics, pp 203-205.

51

The acoustic compliance is:

$$C = \frac{V_g}{\rho_g\, c_g^2}$$

Equating the reactances due to the inertance and compliance and solving for the resonant angular frequency:

$$\omega_c = \sqrt{\frac{1}{MC}} = \sqrt{\frac{S^2\, c_g^2\, \rho_g}{\rho_w\, V_w\, V_g}}$$

As the transducer is lowered in depth we can expect the following effects:

1. The volume of gas decreases.

2. The density of the gas increases.

3. The velocity of sound in the gas remains constant.

4. The volume of water increases.

5. The density of water remains constant.

Solving for f_o, and substituting for S^2 :

$$f_c = \frac{a^2\, c_g}{2\, \rho_w^{1/2}} \sqrt{\frac{\rho_g}{V_w - V_g}}$$

$$V_w = V - V_g$$

From the gas laws with temperature assumed constant during lowering of the transducer:

$$V_g = V_{og}\frac{P_o}{P}, \quad V_w - V_g = V_{cg}\frac{P_o}{P}\left(V - V_{og}\frac{P_o}{P}\right)$$

$$\rho_g = \rho_{og}\frac{P}{P_o}$$

$$f_o = \frac{a^2 C_g}{2\rho_w^{1/2}}\sqrt{\frac{\rho_{og}\frac{P}{P_o}}{V_{cg}\frac{P_o}{P}\left(V - V_{og}\frac{P_o}{P}\right)}}$$

$$f_o = \frac{a^2 C_g \rho_{og}^{1/2}}{2\rho_w^{1/2}}\left(\frac{P}{P_o}\right)\frac{1}{\sqrt{V_{cg}\left(V - V_{og}\frac{P_o}{P}\right)}}$$

To find functional relationships it is convenient to consider one variable at a time holding all others constant. Eliminating constants of proportionality and solving for the resonant frequency as a function of pressure:

$$f \sim \left(\frac{P}{P_o}\right)\frac{1}{\sqrt{\frac{V}{V_{cg}} - \frac{P_o}{P}}}$$

It can be seen that $\frac{P}{P_o}$ will always be greater than unity. As a close approximation frequency will have slightly less than a first power relation to $\frac{P}{P_o}$ if $\frac{V}{V_{og}}$ is large compared to $\frac{P_o}{P}$. In the experiments conducted this was found to be true so that the approximate relation between resonant frequency and hydrostatic pressure is:

$$f_o \sim \frac{P}{P_o}$$

Several spectra which show sufficiently distinct final frequencies that they may be compared to the resonant frequency of a Helmholtz Resonator have been selected for calculations using the formula:

$$f_o = \frac{a^2 c_g \rho_{og}^{1/2}}{2 \rho_w^{1/2}} \left(\frac{P}{P_c} \right) \frac{1}{\sqrt{V_{og} \left(V - V_{og} \frac{P_o}{P} \right)}}$$

$\rho_w = 1.02$

$\rho_{og} = 1.25 \times 10^{-3}$ for N_2. $c_g = 3.37 \times 10^4$ cm/sec for N_2.

$\rho_{og} = 1.43 \times 10^{-3}$ for O_2. $c_g = 1.27 \times 10^5$ cm/sec for H_2.

$\rho_{og} = 8.99 \times 10^{-5}$ for H_2. $c_g = 3.17 \times 10^4$ cm/sec for O_2.

The constants used in making the resonant frequency calculations are listed for reference.

Table 2

COMPARISON OF HELMHOLTZ RESONATOR FREQUENCIES WITH SELECTED
SPECTRA

Transd. Volume	Transd. Radius	Excess Gas	Gas Volume	Depth	Calc. Frequency	Meas. Frequency	Figure No.
6.45 l.	8.25 cm	N_2	3.0 l.	150 ft.	55 cps	57 cps	12(c)
6.45	8.25	N_2	3.0	200	68	73	12(d)
6.45	8.25	H_2	2.0	100	48	56	2(d)
6.45	8.25	N_2	1.0	100	67	70	6(b)
6.45	8.25	O_2	0.74	50	49	45	18(c)
7.30	9.05	O_2	0.74	50	49	50	18(a)
22.8	10.8	O_2	0.74	50	43	40	18(b)

The results of the calculations are listed in Table 2 for comparison
with the frequencies measured from the spectra.

Certain assumptions have been made in the use of the formula for
resonant frequency. The end effects of the transducer opening and the
effect of damping on the resonant frequency have been neglected. Also
it has been assumed that after burning is complete the gas cools rapidly
to the temperature of the surrounding water. The frequency shift is
assumed to correspond to the time when the gas has cooled, and the
Helmholtz Resonator frequency is compared to the frequency after the
shift.

10. Conclusions and Recommendations

The following conclusions were based upon the experimental data collected and the frequency analysis.

a. The presence of an excess gas bubble in the container of the explosive mixture causes the acoustic output of the explosion to form discrete frequency components.

b. Different quantities of the excess gas did not cause significant changes in the frequencies at which the discrete components appeared. This is consistent with a Helmholtz Resonator explanation of the frequency production.

c. When large amounts of excess gas were used, the frequency spectra contained only one or two single frequency components. Excess hydrogen produced higher frequencies than did excess nitrogen, also in agreement with a Helmholtz Resonator explanation.

d. Increasing depth, or in other words static pressure, caused an upward shift of frequencies with approximately a first power relationship between frequency and hydrostatic pressure.

e. Increasing depth produces a broadening of the spectrum introducing higher frequency components.

f. Reflection from the surface modifies the spectrum considerably. At a depth of 50 feet or less where reflection is strong, and the time corresponding to the path difference between the direct and reflected

wave is shorter than the pulse duration, results will be erratic.

g. The frequency shifts upward during the pulse. A pulse begins with a short oscillation of one frequency and then, after reaching maximum amplitude, the frequency jumps up to a higher value.

h. The frequency of oscillation after the frequency shift has occurred agrees with the frequency calculated considering the transducer as a gas and water filled Helmholtz Resonator.

A gas filled transducer can be employed as a relatively pure source of low frequency sound. The frequency can be selected in the construction of the transducer. Frequency is a function of the square of the radius of the transducer providing a very convenient means of putting the frequency in a useful range.

The authors make the following recommendations:

a. Work in this field should be continued. An experimental transducer of larger size and radius should be constructed. The resulting output should have the advantages of more power out and a higher frequency range. Measurements should be made to determine whether or not such a device will also operate as a Helmholtz Resonator when a large quantity of excess gas is present. Acquisition and calibration of instruments for accurate measurement of peak power should be attempted.

b. Measurements should be extended to deeper water. This would include assignment of a larger boat to the project since the 40 foot

motor launch used can only be operated within a limited radius of base.

c. Work on the production of hydrogen and oxygen by electrolysis of sea water should be carried out for fast charging rates. This method of producing the explosive mixture shows the most promise for very deep shots if the rate of gas production can be increased sufficiently.

d. The feasibility of employing such a device for long range communications or echo ranging in the deep sound channels should be considered.

e. The frequency spectrum analyzer developed for this project can be employed in its present form for the analysis of future data. It can also be modified for use in connection with other projects. A valuable improvement would be to increase the dynamic range. In its present form the Frequency Analyzer is linear over the 25 decibel range and the 25 decibel potentiometer is used with the Bruel & Kjaer Level Recorder. Potentiometers for 50 and 75 decibel ranges are available for the Level Recorder, but in order to use them the Amplifier – Detector would have to be redesigned to increase the linear range.

BIBLIOGRAPHY

1. H. Wilson and C. I. Mathews, Some Experimental Sound Sources, Underwater Sound Laboratory Report No. 267, 1955.

2. J. R. Harris and C. M. Rigsbee, An Investigation of the Power Spectrum of Underwater Explosions of Gaseous Hydrogen and Oxygen, U. S. Naval Postgraduate School, 1960.

3. V. I. Sorokin, Investigation of Water-Air Resonators, Soviet Physics (Acoustics) Vol. 4 No. 2, Pgs. 188-195, April-June 1958.

4. L. E. Kinsler and A. R. Frey, Fundamentals of Acoustics, John Wiley & Sons Inc., 1950.

5. R. H. Cole, Underwater Explosions, Princeton University Press, 1950.

APPENDIX I

FREQUENCY SPECTRUM ANALYZER

A system was designed and assembled to satisfy the requirements
for a precision low frequency spectrum analyzer. The frequency analyzer
had the capability of analyzing a short duration non-periodic voltage
function of time, such as the voltage output of a hydrophone produced
by an underwater explosion. The output was a graphical plot of the
relative 2.25 cycle band level in decibels as a function of frequency.
The dynamic range of the system was 25 decibels. The selectivity was
2.25 cycles per second. As employed by these writers the system pro-
vided a presentation of relative sound pressure spectrum level from 20
to 2500 cycles per second. In this range the system was flat within
two decibels. (See Figure 28.)

The narrow bandwidth of 2.25 cycles per second was achieved
by recording the signal on magnetic tape, playing it back at a faster
speed to provide frequency multiplication, and then passing the signal
through a highly selective wave analyzer. The non-periodic signal was
made into a long-period periodic signal by making a closed loop of the
tape and playing it continuously. The repeated signal was played through
a slowly swept filter. The output of the filter was integrated for each
repetition and the integrator output recorded as the 2.25 cycle band
level.

The fact that a non-periodic function was being converted into a periodic function did not detract from the validity of the analysis. If we consider a single rectangular pulse, it has a continuous frequency spectrum, the envelope of which is a $\frac{\sin x}{x}$ distribution. If the pulse length is t_O then the first null of the $\frac{\sin x}{x}$ distribution is for the frequency $f = \frac{1}{t_O}$. Now consider an infinite train of such pulses each of length t_O and arriving with frequency $f_1 = \frac{1}{t_1}$. We now have a periodic function of period t_1. The spectrum still has the $\frac{\sin x}{x}$ distribution of the envelope but it is no longer continuous, it has components only at frequencies $f = nf_1$ where n is an integer. In this system t_1 was made one second so components occurred only at one cycle intervals on the frequency scale. Because the bandwidth of the filter in this case was 18 cycles per second the filter was unable to resolve the one cycle component separation. Thus the output of the system analyzing the long-period periodic function is indistinguishable from that of the non-periodic function.

The hydrophone output was recorded on an Ampex 600 tape recorder at a speed of 7.5 inches per second. (Refer to Figure 21.) The piece of tape with the short explosion was made into a loop and was played back at 60 inches per second on an Ampex S-3108 tape recorder. All frequencies were thereby multiplied by a factor of eight. After this frequency multiplication an 18 cycle per second bandwidth corresponded to a 2.25

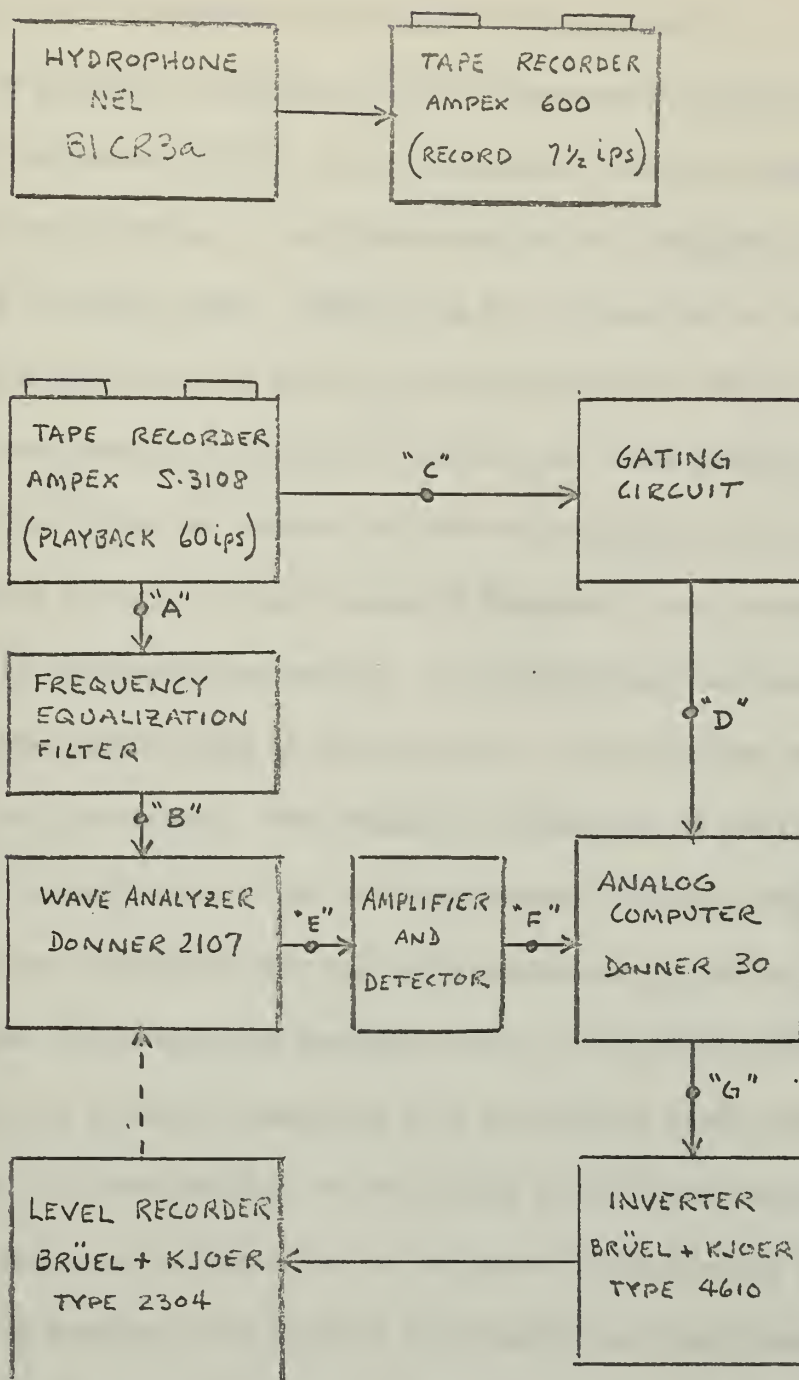Fig. 21 Spectrum Analyzer, Functional Block Diagram

cycle per second bandwidth at the original frequencies.

The frequency equalization filter compensated for the unequal frequency emphasis resulting from the recording and high speed playback of the two tape recorders. The filter consists of a high pass filter followed by a low pass filter. (See Figure 22.) The output of the frequency equalization filter was fed into the Donner model 2107 Wave Analyzer. The wave analyzer has a selectivity curve down three decibels at plus or minus nine cycles per second and down 40 decibels at plus or minus 40 cycles per second. It has a range of frequency from 30 cycles per second to 50 kilocycles per second. The frequencies measured in this series of experiments were in the range from 160 cycles per second to 16 kilocycles per second. The frequency calibration of the Donner Wave Analyzer is normally plus or minus three percent plus ten cycles per second but the instrument was specially calibrated in the low frequency range for use in the spectrum analysis set up. The Donner Wave Analyzer was swept very slowly in frequency by a mechanical shaft from the Bruel & Kjaer type 2304 Level Recorder to the tuning shaft of the Donner Wave Analyzer. Referring to Figure 24, a functional block diagram of the Donner Wave Analyzer, the shaft of the tunable local oscillator was turned by the mechanical linkage. The crystal filters in the IF section provide the selectivity previously mentioned. The output of the second IF amplifier was tapped off at the plate of V-4 and fed to the amplifier-detector.
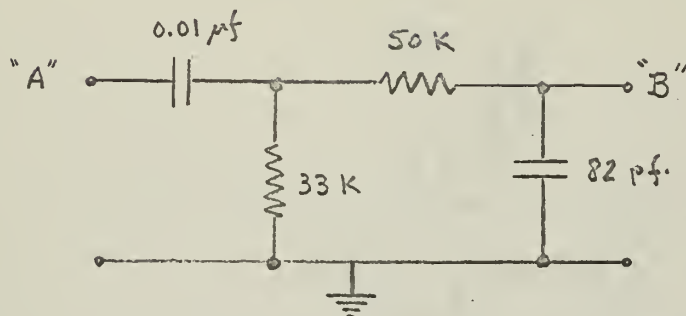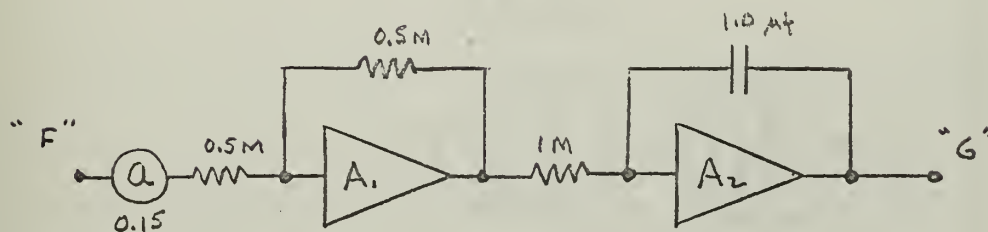
: Fig. 22 Frequency Equalization Filter

Fig. 23 Analog Computer Set-Up
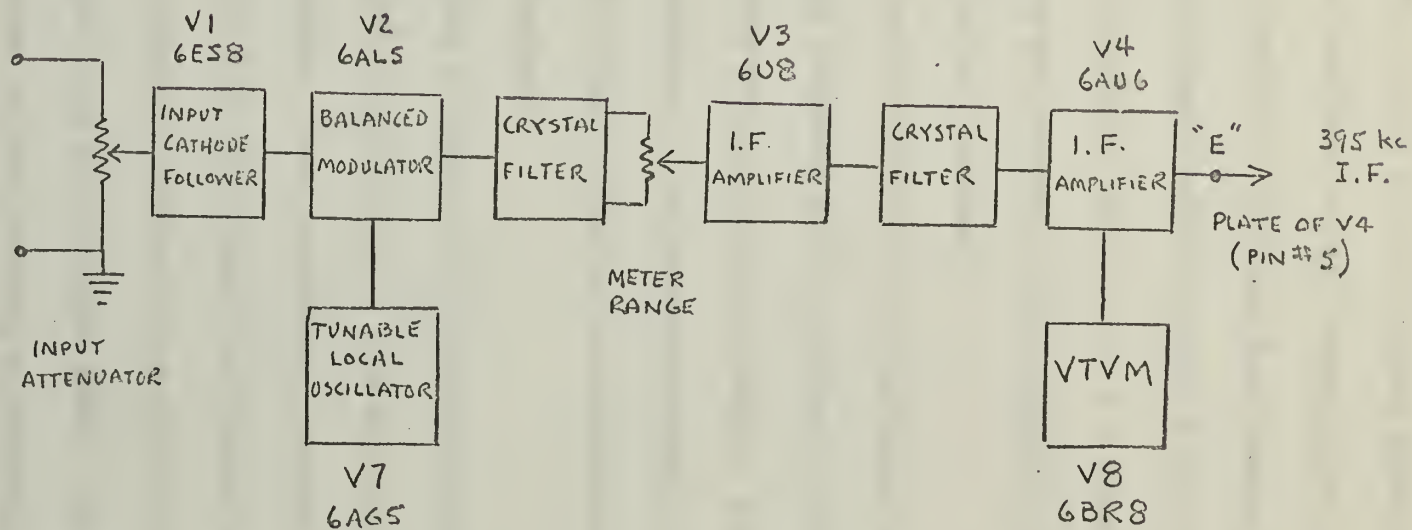
Fig. 24   Functional Block Diagram of Donner 2102 Wave Analyzer

The amplifier-detector (Refer to Figure 25.) provides a DC voltage proportional to the amplitude of the IF from the Donner Wave Analyzer. V-1 of the amplifier-detector amplifies the 395 kilocycle per second IF. V-2 is a cathode follower to prevent the detector from loading the amplifier V-1. V-3 is an envelope detector which provides a DC output to the integrator. The 1.5 volt battery in the circuit of V-3 cancels the contact potential of the diode and provides a small amount of thresholding to eliminate noise from the integrator.

The output of the detector is integrated on the Donner model 30 Analog Computer. The Analog Computer set up is shown in Figure 23. The function of A_1 is to provide the proper polarity output. The amplifier A_2 is a highly stable integrator. The integration cycle is controlled by the gating circuit which provides a signal to the computer-reset input at the back of the Analog Computer.

The gating circuit (Refer to Figure 26.) takes the audio signal from the Ampex S-3108, amplifies it in V-4a and V-4b and uses it to trigger a monostable multivibrator. V-5a is a diode to provide a negative trigger to the plate of V-6a, the normally off tube of the delay multivibrator. The negative trigger is coupled to the grid of the on tube, V-6b, causing the multivibrator to go to its astable state. The time constant of the delay is adjusted so that the delay multivibrator returns to its stable state just prior to the next audio pulse from the tape recorder.
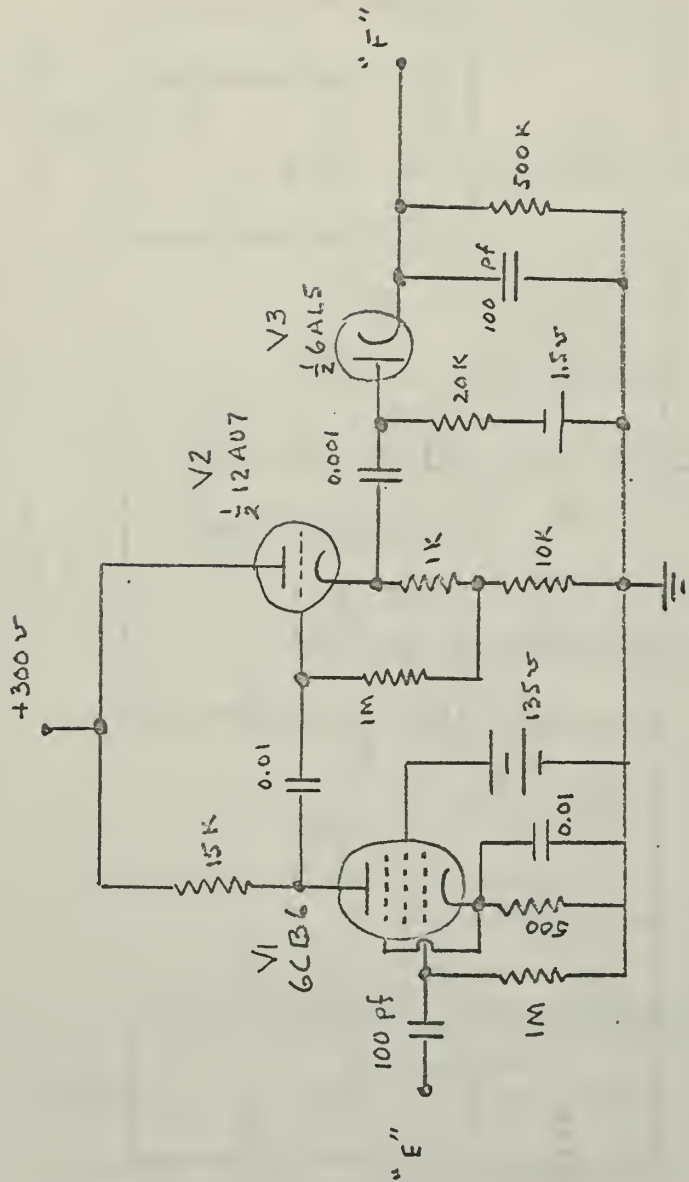
Fig. 25 Amplifier and Detector

Fig. 26 Gating Circuit
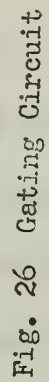
The return of the delay multivibrator to its stable state provides a negative trigger for the second multivibrator which is the gate multivibrator. The gate multivibrator, V-7a and V-7b, operates in the same way as the previous multivibrator. A positive gate appears at the plate of V-7b. The 45 volt battery in the cathode circuit of V-8 holds the cathode of V-6 negative with respect to ground except when the positive gate from the plate of V-7b causes V-8 to conduct. At that time the cathode of V-8 goes to plus five volts. The Analog Computer integrates for the duration of this positive gate.

A dual channel oscilloscope is useful for adjusting the two multivibrators. The audio signal applied to one channel and the integrator gate applied to the other channel superimposes the two for easy adjustment. The time constant of the gate multivibrator is adjusted for the proper integration time, and the time constant of the delay multivibrator is adjusted to position the audio signal pulse in the center of the gate. It is convenient to trigger the scope with the leading edge of the gate.

The output of the integrator is fed to the Bruel & Kjaer type 4610 Inverter. The inverter is a 400 cycle per second chopper which provides an AC signal to the Bruel & Kjaer type 2304 Level Recorder. The Level Recorder will not operate on a DC input. The Bruel & Kjaer Level Recorder is particularly useful as an indicator for the system. It has a moving

paper tape which is scratched by a needle. The needle moves to a level proportional to the voltage out of the integrator. The Level Recorder has a mechanical output which was used as a drive for the shaft of the Donner Wave Analyzer. The shaft of the Donner Wave Analyzer was made to move in synchronism with the traveling tape on the Level Recorder. The mark button was pressed on the Bruel & Kjaer Recorder as the dial on the Donner Wave Analyzer passed the marks corresponding to the frequency being passed.

As a precaution to ensure linearity of the system the voltage at point "F" (See Figure 21.) should be monitored with an oscilloscope. The input attenuator on the Donner Wave Analyzer should be adjusted so that the peak voltage at the point "F" does not exceed plus 20 volts. Also point "G" should be monitored and the input attenuator on the Analog Computer adjusted so that the maximum voltage at point "G" does not exceed plus 300 millivolts.

Figure 27 shows the spectral analysis of some test signals recorded to test the performance of the system. Figure 27a is the analysis of a 440 millisecond pulse of a 70 cycle per second sine wave. The $\frac{\sin x}{x}$ distribution is centered at 70 cycles per second and the first null should be at 2.25 cycles per second away from the center frequency. Note the first null is not distinguishable in this picture. Figure 27b is the analysis of a 30 millisecond pulse of a 300 cycle per second sine wave.

Test pulse
70 cps sine wave
Pulse length 440 ms

Test pulse
300 cps sine wave
Pulse length 30 ms

Linearity test:
Steady state sine
wave attenuated
in 5 db steps
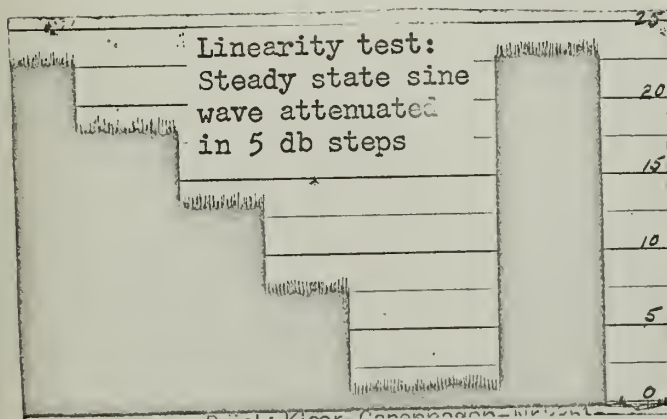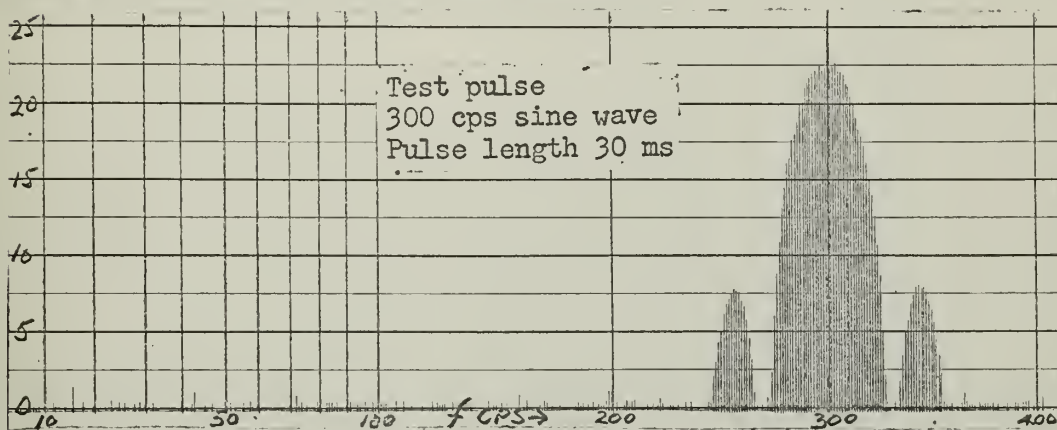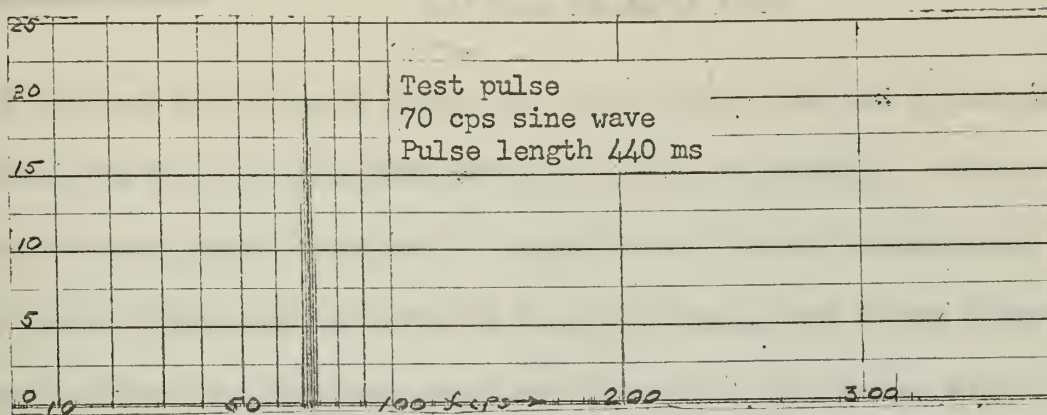
Fig. 27   Spectrum Analyzer Tests

The first null should be 33 cycles per second away from 3oo cycles per second and the first side lobes should be down 14 decibels. The experimental results check quite well. Figure 27c is a steady signal input to the Donner Wave Analyzer with the frequency attenuated in five decibel steps to check the combined amplitude linearity of the Donner Wave Analyzer, the amplifier - detector, the integrator, the Bruel & Kjaer Inverter and the Bruel & Kjaer Level Recorder.
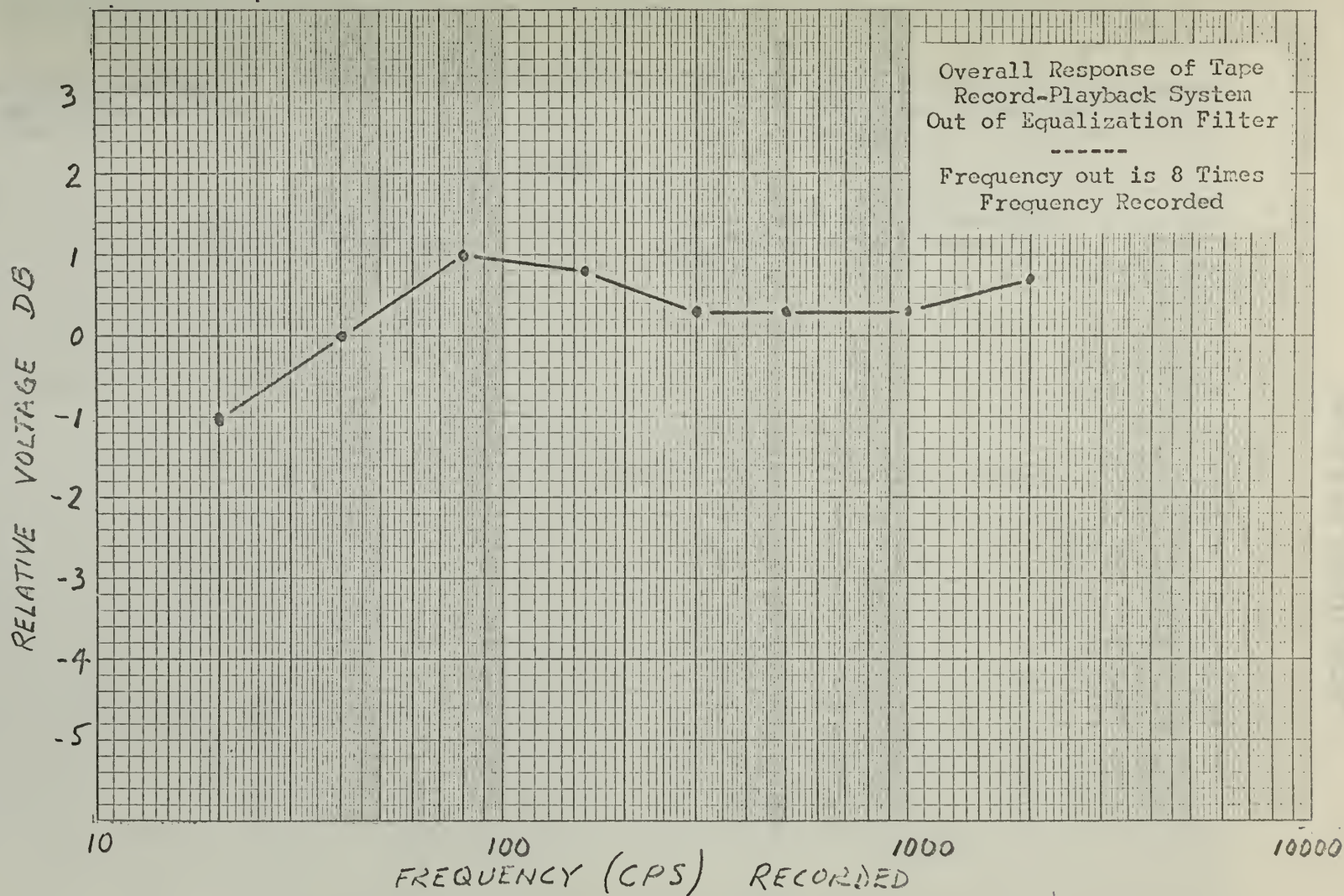
Fig. 28 Overall Response of Tape Record-Playback System
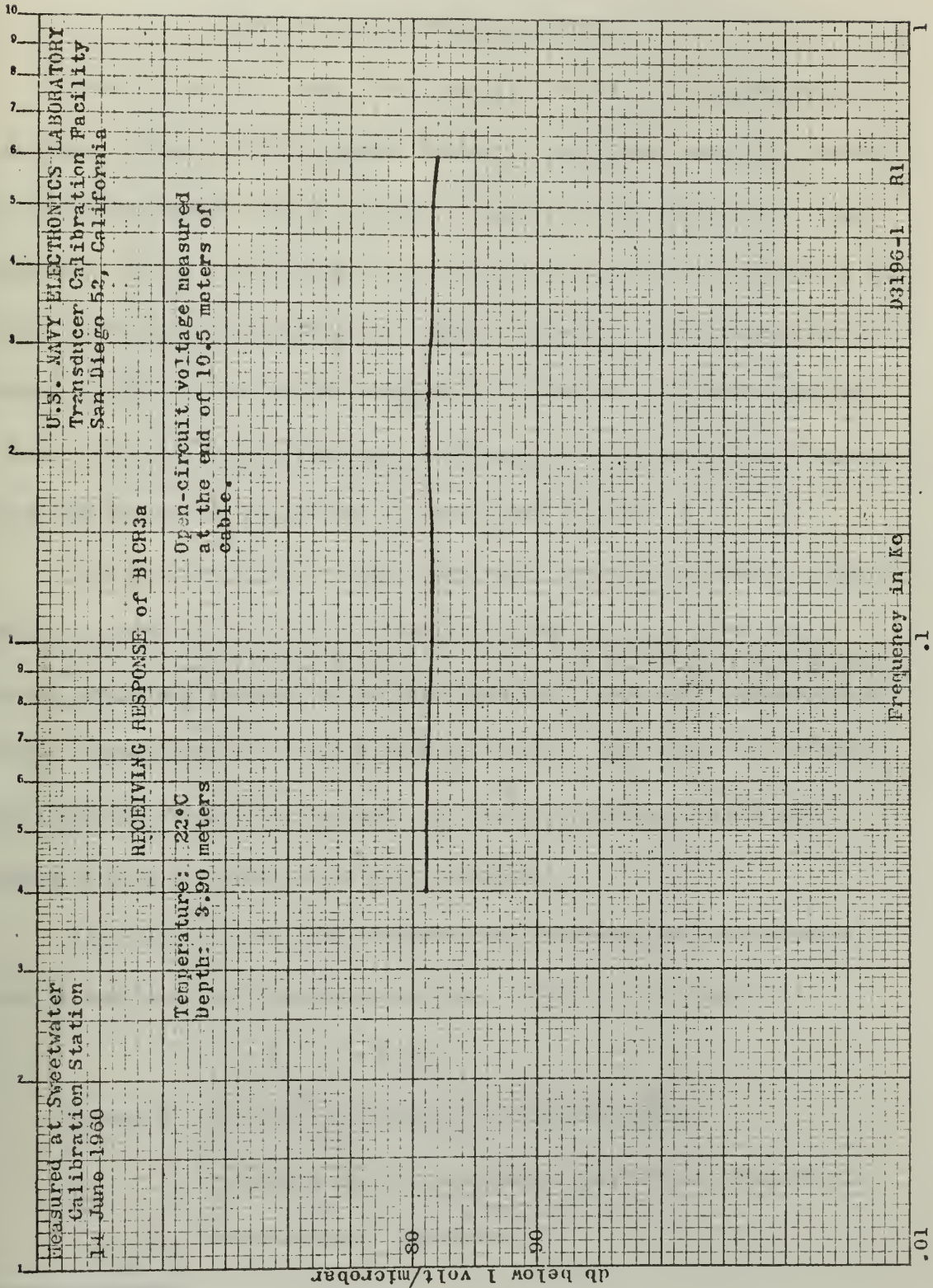
Fig. 29 Hydrophone Response

APPENDIX II

GAS VOLUME MEASUREMENTS

The transducers were loaded with gas from tanks of compressed hydrogen, oxygen, and nitrogen. Pressure regulators were installed on the tanks and hoses were connected to the pressure regulators. The other ends of the hoses were connected to the applicator wand made up of three lengths of copper tubing. (See Figure 30.) The transducer was placed immediately below the surface of the water and inverted briefly to empty it of air. Then the applicator wand was placed under the transducer and measured quantities of gases were bubbled in.

The precise amount of each gas was measured by means of the pressure gauge on the tank. Initially the low pressure valve was closed, and the pressure on the high pressure gauge was brought up to a value determined from the calibration curve. (See Figure 31.) Then, with the high pressure valve shut off, the low pressure valve was opened to bubble the gas into the transducer.

The calibration curves for the three pressure regulators were made in advance from experimental data. From the gas laws:

$$P_1 V_1 = P_2 V_2$$

where P_1 = Pressure on the high pressure gauge.

V_1 = Volume of gas trapped in the pressure regulator.

P_2 = Atmospheric pressure.

(a) Measuring Valves and Gas Bottles

(b) Applicator and Hoses

Fig. 30 Gas Measuring Apparatus
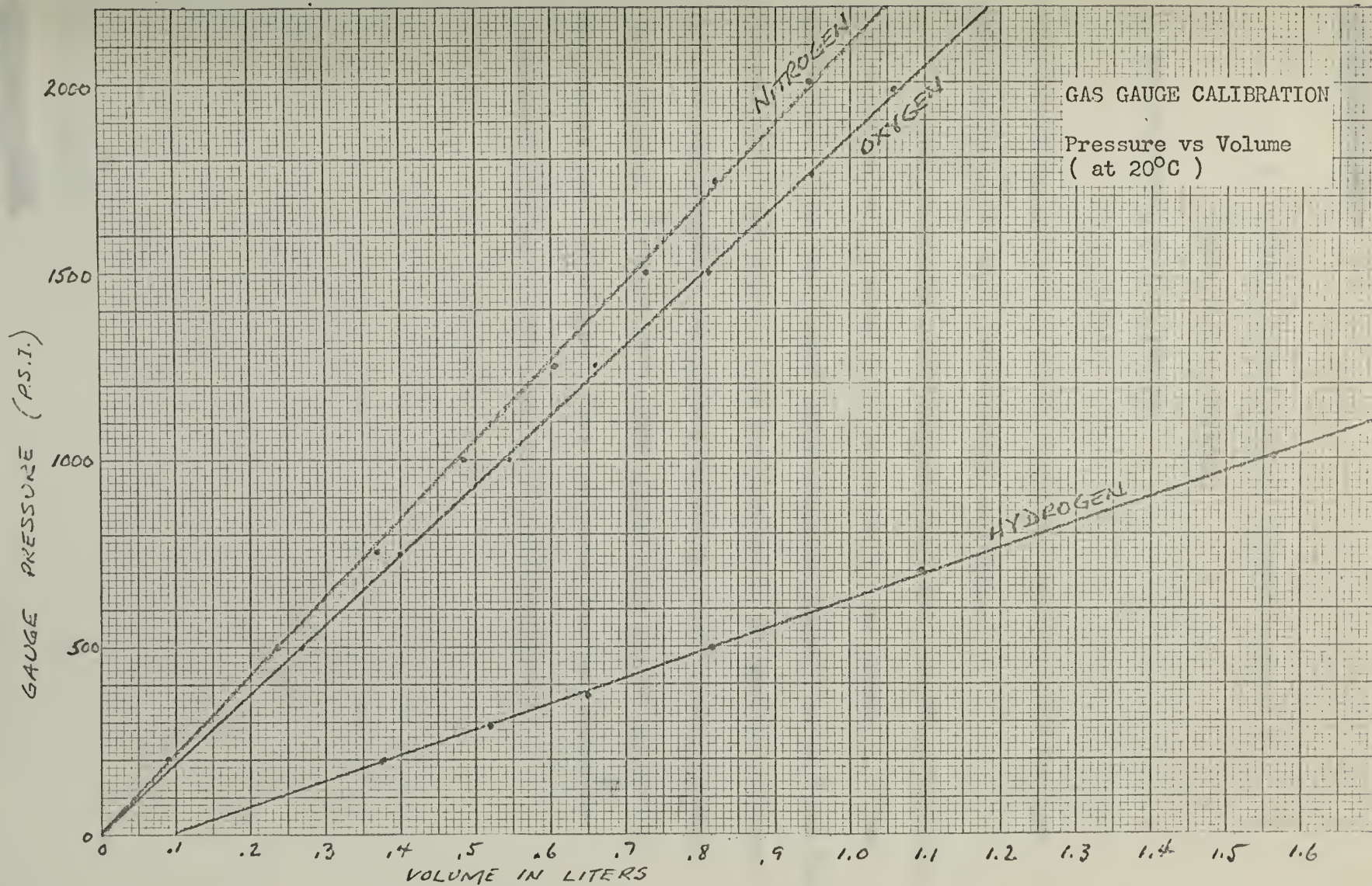
Fig. 31 Gas Gauge Calibration

V_2 = Volume of gas inserted in the transducer at

atmospheric pressure.

V_1 was not known so the relation

$$V_2 = K\,P_1$$

was plotted experimentally at 20° C and the resulting curve for each

gas was consulted when the transducer was loaded.

A test was performed to determine how much gas dissolved when

the transducer was lowered to the firing depth. An inverted 1.0 liter

graduated cylinder was loaded with a measured quantity of each gas and

lowered to 200 feet depth. After five minutes at 200 feet the graduated

cylinder was brought to the surface and the quantity of gas remaining

was measured. For each of the three gases there was no perceptible

loss of gas due to dissolving. Gas volumes in the transducers are

considered accurate to within plus or minus 20 milliliters.

APPENDIX III

DESCRIPTION OF TRANSDUCERS

The transducers used in the experiments all were of the same basic design, that is they consisted of steel cylinders closed at the top and open at the bottom. A nichrome wire was mounted at the top of each cylinder for ignition of the explosive mixture. A harness attached to the top of each cylinder was used for connecting a line for raising and lowering the transducers. Twin conductor Romex cable connected a 24 volt storage battery from the boat to the nichrome glow wire. Proper adjustment of a series resistor limited the glow wire current to 15 amperes, the maximum allowable without destroying the glow wire.

The diameters of the steel cylinders were chosen because of convenient steel stock available or because of construction by our predecessors in the field, Harris and Rigsbee. The intent was to observe the effects of different transducer cross sections and sizes rather than to produce a specific design.

As a convenience for reference in the Tabulation of Explosions, Appendix V, the transducers have been numbered. The transducers are shown in Figure 32 for which the data below applies.

Fig. 32	Transd. No.	Volume (liters)	Inside Radius(cm)
(a)	1	7.30	9.05
(b)	2	22.8	10.8
(c)	3	4.03	2.62
(d)	4	6.45	8.25

(a) 7.30 Liter Transducer
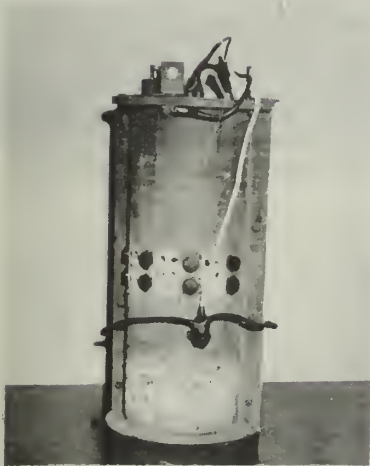
(b) 22.8 Liter Transducer

Fig. 32 Transducers

(c) 4.03 Liter Transducer

(d) 6.45 Liter Transducer

(e) Cap and Ignition Wire

Fig. 32 Con't.

APPENDIX IV

SPECTRUM BROADENING DUE TO REFLECTION

Consider the frequency spectrum of a cosine pulse of frequency

$f_0 = \dfrac{\omega_0}{2\pi}$ and duration $\dfrac{T}{2}$ as shown below:
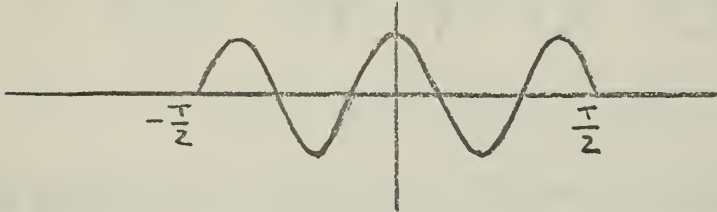
The amplitude as a function of time is:

$$f(t) = \begin{cases} \sin \omega_0 t & \text{for} \quad -\dfrac{T}{2} \le t \le \dfrac{T}{2} \\ 0 & \text{for} \quad |t| > \dfrac{T}{2} \end{cases}$$

Take the Fourier Transform:

$$F(\omega) = \int_{-\frac{T}{2}}^{\frac{T}{2}} \cos \omega_0 t \; e^{-j\omega t} dt = \int_{-\frac{T}{2}}^{\frac{T}{2}} \frac{e^{j\omega_0 t} + e^{-j\omega_0 t}}{2} e^{-j\omega t} dt$$

$$F(\omega) = -\left[\frac{e^{-j(\omega-\omega_0)t}}{2j(\omega-\omega_0)} \right]_{-\frac{T}{2}}^{\frac{T}{2}} - \left[\frac{e^{-j(\omega+\omega_0)t}}{2j(\omega+\omega_0)} \right]_{-\frac{T}{2}}^{\frac{T}{2}}$$

$$F(\omega) = -\frac{e^{-j(\omega-\omega_0)\frac{T}{2}} - e^{j(\omega-\omega_0)\frac{T}{2}}}{2j(\omega-\omega_0)} - \frac{e^{-j(\omega+\omega_0)\frac{T}{2}} - e^{j(\omega+\omega_0)\frac{T}{2}}}{2j(\omega+\omega_0)}$$

$$F(\omega) = \frac{T}{2} \frac{\sin(\omega-\omega_0)\frac{T}{2}}{(\omega-\omega_0)\frac{T}{2}} + \frac{T}{2} \frac{\sin(\omega+\omega_0)\frac{T}{2}}{(\omega+\omega_0)\frac{T}{2}}$$

The first term contains the positive frequencies.

Now consider the spectrum of the pulse below. It is an idealized cosine pulse immediately followed by its negative reflection.
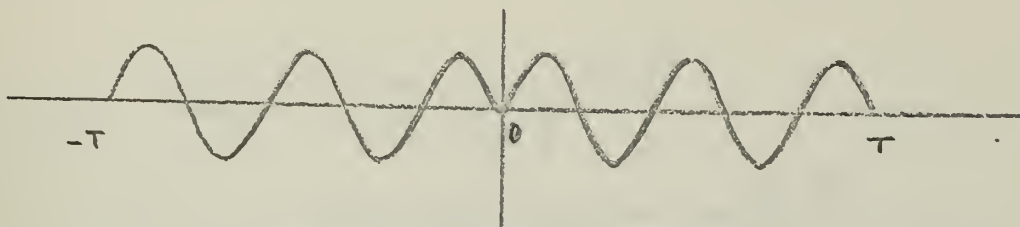
The amplitude as a function of time for this pulse is:

$$f(t) = \begin{cases} \sin \omega_o t & \text{for } 0 \le t \le T \\ -\sin \omega_o t & \text{for } -T \le t \le 0 \\ 0 & \text{for } |t| > T \end{cases}$$

Again take the Fourier Transform:

$$F(\omega) = \int_{-T}^{0} (-\sin \omega_o t) e^{-j\omega t} dt + \int_{0}^{T} \sin \omega_o t \, e^{-j\omega t} dt$$

$$F(\omega) = \int_{-T}^{0} \frac{e^{-j\omega_o t} - e^{j\omega_o t}}{2j} e^{-j\omega t} dt + \int_{0}^{T} \frac{e^{j\omega_o t} - e^{-j\omega_o t}}{2j} e^{-j\omega t} dt$$

$$F(\omega) = \left[\frac{e^{-j(\omega+\omega_o)t}}{2(\omega+\omega_o)}\right]_{-T}^{0} - \left[\frac{e^{-j(\omega-\omega_o)t}}{2(\omega-\omega_o)}\right]_{-T}^{0} + \left[\frac{e^{-j(\omega-\omega_o)t}}{2(\omega-\omega_o)}\right]_{0}^{T} - \left[\frac{e^{-j(\omega+\omega_o)t}}{2(\omega+\omega_o)}\right]_{0}^{T}$$

$$F(\omega) = \frac{1 - e^{j(\omega+\omega_o)T}}{2(\omega+\omega_o)} - \frac{1 - e^{j(\omega-\omega_o)T}}{2(\omega-\omega_o)} + \frac{e^{-j(\omega-\omega_o)} - 1}{2(\omega-\omega_o)} - \frac{e^{-j(\omega+\omega_o)T} - 1}{2(\omega+\omega_o)}$$

$$F(\omega) = \frac{1 - \cos(\omega+\omega_o)T}{\omega+\omega_o} - \frac{1 - \cos(\omega-\omega_o)T}{\omega-\omega_o}$$

$$F(\omega) = \frac{2 \sin^2 (\omega+\omega_o)\frac{T}{2}}{\omega+\omega_o} - \frac{2 \sin^2(\omega-\omega_o)\frac{T}{2}}{\omega-\omega_o}$$

$$F(\omega) = \frac{(\omega+\omega_0)T^2}{2}\left[\frac{\sin{(\omega+\omega_0)\frac{T}{2}}}{(\omega+\omega_0)\frac{T}{2}}\right]^2$$

$$- \frac{(\omega-\omega_0)T^2}{2}\left[\frac{\sin{(\omega-\omega_0)\frac{T}{2}}}{(\omega-\omega_0)\frac{T}{2}}\right]^2$$

Here the second term contains the positive frequencies.

In the first case under consideration the simple cosine pulse has a $\frac{\sin x}{x}$ distribution of the spectrum with the maximum amplitude of the spectrum at ω_0. In the second case where reflection exists there will be no component at ω_0.

Next let us consider the components corresponding to $x = \frac{3\pi}{2}$ in the $\frac{\sin x}{x}$ distribution. They occur when:

$$\left(\omega - \omega_0\right)\frac{T}{2} = \frac{3\pi}{2}, \quad \frac{\sin\frac{3\pi}{2}}{\frac{3\pi}{2}} = 0.2, \quad \left[\frac{\sin x}{x}\right]^2 = 0.04$$

The amplitude of the spectral component for the simple cosine pulse of the first case will be:

$$A = \frac{T}{2}\frac{\sin x}{x} = 0.2\left(\frac{T}{2}\right)$$

The amplitude of the spectral component where reflection occurs as in the second case is:

$$A = \frac{(\omega-\omega_0)T^2}{2}\left[\frac{\sin x}{x}\right], \quad \text{since} \quad T = \frac{3\pi}{\omega-\omega_0}$$

$$A = 3\pi\left(\frac{T}{2}\right)(0.04), \quad A = 0.377\left(\frac{T}{2}\right)$$

The result is an increase of 5.5 decibels for the second case over the first case.

Consider the component corresponding to $x = \dfrac{5\pi}{2}$ in the $\dfrac{\sin x}{x}$ distribution. They occur when:

$$\left(\omega - \omega_0\right)\frac{T}{2} = \frac{5\pi}{2} \;,\quad \frac{\sin\frac{5\pi}{2}}{\frac{5\pi}{2}} = 0.12 \;,\quad \left[\frac{\sin x}{x}\right]^2 = 0.0144$$

For the cosine pulse the amplitude of the spectral component will be:

$$A = \frac{T}{2}\frac{\sin x}{x} = 0.12\left(\frac{T}{2}\right)$$

For the reflected pulse plus incident pulse of the second case, the amplitude of the component will be:

$$A = \frac{\left(\omega - \omega_0\right)T^2}{2}\left(\frac{\sin x}{x}\right)^2 \;,\quad \text{since}\quad T = \frac{3\pi}{\omega - \omega_0}$$

$$A = 5\pi\left(\frac{T}{2}\right)\left(0.0144\right) \;,\quad A = 0.226\left(\frac{T}{2}\right)$$

A comparison again shows an increase of 5.5 decibels caused by reflection.

The example considered is a simplified ideal case. But it can readily be seen that a phase reversed reflection, such as from the surface, arriving with the proper time relation to the direct wave can suppress the spectral component ω_0 and enhance the other frequency components.

APPENDIX V

TABULATION OF EXPLOSIONS

Shot Number	Transducer Number	Transducer Depth (ft)	Hydrophone Depth (ft)	Gas Volumes (liters)	
				H_2	O_2
1	1	5	15	0.65	1.06
2	1	15	15	0.65	1.06
3	1	50	50	0.65	1.06
4	1	50	50	0.65	1.06
5	1	50	50	0.65	1.06
6	1	50	25	0.65	1.06
7	1	50	25	0.65	1.06
8	1	50	75	0.65	1.06
9	1	50	75	0.65	1.06
10	missing				
11	2	50	50	0.65	1.06
12	3	150	150	0.67	0.33
13	3	150	150	0.75	0.25
14	3	150	150	0.80	0.20
15	3	150	150	0.83	0.17
16	3	150	150	0.86	0.04
17	3	150	150	0 88	0.12
18	3	150	150	0.89	0.11

Shot Number	Transducer Number	Transducer Depth (ft)	Hydrophone Depth (ft)	Gas Volumes (liters)		
				H_2	O_2	N_2
19	3	150	150	2.67	0.33	
20	3	150	150	0.50	0.50	
21	3	150	150	0.33	0.67	
22	3	150	150	0.50	1.50	
23	3	150	150	0.40	1.60	
24	3	150	150	2.00	1.00	
25	3	150	150	2.40	0.60	
26	3	50	50	0.67	0.33	
27	3	50	50	1.33	0.33	
28	3	100	100	0.67	0.33	
29	3	100	100	1.33	0.33	
30	3	150	150	0.67	0.33	
31	3	150	150	1.33	0.33	
32	3	200	200	0.67	0.33	
33	3	200	200	1.33	0.33	
34	4	50	50	0.67	0.33	
35	4	50	50	1.33	0.33	
36	4	50	50	2.00	1.00	
37	4	100	100	0.67	0.33	
38	4	100	100	1.33	0.33	

Shot Number	Transducer Number	Transducer Depth (ft)	Hydrophone Depth (ft)	Gas Volumes (liters)		
				H_2	O_2	N_2
39	4	100	100	2.00	0.33	
40	4	100	100	2.67	0.33	
41	4	100	100	4.00	0.67	
42	4	150	150	0.67	0.33	
43	4	150	150	1.33	0.33	
44	4	150	150	2.00	0.33	
45	4	150	150	2.67	0.33	
46	4	150	150	4.00	0.67	
47	4	200	200	0.67	0.33	
48	4	200	200	1.33	0.33	
49	4	200	200	2.00	0.33	
50	4	200	200	2.67	0.33	
51	4	200	200	4.00	0.67	
52	4	50	50	0.67	0.33	
53	4	50	50	0.67	0.33	1.00
54	4	50	50	0.67	0.33	2.00
55	4	50	50	0.67	0.33	3.00
56	4	50	50	1.67	0.33	
57	4	50	50	2.67	0.33	
58	4	50	50	3.67	0.33	

Shot Number	Transducer Number	Transducer Depth (ft)	Hydrophone Depth (ft)	Gas Volumes (liters)		
				H_2	O_2	N_2
59	4	100	100	0.67	0.33	
60	4	100	100	0.67	0.33	1.00
61	4	100	100	0.67	0.33	2.00
62	4	100	100	0.67	0.33	3.00
63	4	100	100	1.67	0.33	
64	4	100	100	2.67	0.33	
65	4	150	150	0.67	0.33	
66	4	150	150	0.67	0.33	1.00
67	4	150	150	0.67	0.33	2.00
68	4	150	150	0.67	0.33	3.00
69	4	100	100	3.67	0.33	
70	4	150	150	0.67	0.33	3.00
71	4	200	200	0.67	0.33	3.00
72	4	25	25	0.67	0.33	1.33
73	4	50	50	0.67	0.33	1.33
74	4	75	75	0.67	0.33	1.33
75	4	100	100	0.67	0.33	1.33
76	4	125	125	0.67	0.33	1.33
77	4	150	150	0.67	0.33	1.33
78	4	175	175	0.67	0.33	1.33

UNCLASSIFIED

Shot Number	Transducer Number	Transducer Depth (ft)	Hydrophone Depth (ft)	Gas Volumes(liters)		
				H_2	O_2	N_2
79	4	200	200	0.67	0.33	1.33
80	4	50	50	0.65	1.06	